NORTHWESTERN UNIVERSITY

Estimation of Persistent Inward Currents in the Human Ankle Flexor and Extensor Muscles

A DISSERTATION

SUBMITTED TO THE GRADUATE SCHOOL

IN PARTIAL FULFILMENT OF THE REQUIREMENTS

For the degree

DOCTOR OF PHILOSOPHY

Field of Neuroscience

By

Edward Kim

EVANSTON, ILLINOIS

September 2021

ABSTRACT

Movement is achieved by combining synaptic inputs from various sources and activating motor

unit populations. Motor units are the quantal elements of motor control which act as a

neuromechanical transducer that converts sensory inputs into motor output. Because of the

tight neuromuscular junctions between motoneuron axon terminals and a large number of

muscle fibers each motoneuron innervates, synaptic inputs to the motoneuron pool can be

routinely observed as motor unit firing patters via electromyography (EMG) signals. Persistent

inward currents (PICs) are modulated by monoaminergic inputs from the brainstem and

increase the motoneuron excitability. Animal models have shown that PICs play an important

role in normal movement such as balance and postural control. However, the role of PICs in

human motor control and how they affect motor unit firing patterns are not well understood.

Through recent advances in EMG recording technics, researchers can now simultaneously

record many motor units in humans using non-invasive high-density surface EMG arrays.

Combined with a well-established delta-F (ΔF) technique, this dissertation investigated PICs in

human soleus and tibialis anterior muscles (TA). The results showed ΔF was significantly higher

in the TA than the soleus and the trend continued across various effort levels. Surprisingly,

changing effort levels did not affect ΔF's in either of the muscles. The effects of muscle

contraction speed were also studied, and the results showed that it also did not change ΔF.

Lastly, the biases of the EMG decomposition algorithm were discussed, and the results showed

for lower contraction levels and speeds, surface EMG decomposition discriminated a large

number of low-threshold units. However, during at higher contraction speeds and torque levels

the proportion of low threshold motor units decomposed was reduced, resulting in a relatively

uniform distribution of recruitment thresholds. These studies provided valuable insights on PICs

in humans but also revealed how little we understand human motor control. Continuing efforts

are needed to further understand the functional role of PICs in human movement.

ACKNOWLEDGEMENT

First and foremost, I would like to thank my advisor, Dr. CJ Heckman, for his guidance and support throughout the entire duration of my Ph.D. career. It would not have been possible to complete this project without his patience and encouragement. I would also like to thank my committee members, Dr. Jules Dewald, Dr. Nina Suresh, and Dr. Eric Perreault. Dr. Jules Dewald allowed me to use resources at the Department of Physical Therapy and Human Movement Sciences to perform experiments. Dr. Nina Suresh always gave useful insights on data analysis and interpretation. Dr. Eric Perreault kindly explained linear mixed model and helped me with statistical analysis of the results. I would like to extend my gratitude to Dr. Jessica Wilson for training me from the beginning and teaching me how to collect EMG data and analysis. I thank Dr. Christopher Thompson for helping me with collecting intramuscular data and providing any additional help, especially for the second chapter of this thesis. I also thank Dr. Obaid Khurram who played a crucial role in data collection and analysis for the second chapter of this thesis. Lastly, I would like to thank my family who scarified so much, and I wouldn't have been able to complete my Ph.D. without their unconditional support.

TABLE OF CONTENTS

BACKGROUND

History of Motor Unit Recordings in Humans

Motor units are a neuromechanical transducer that converts sensory and descending neural inputs into forces and generates movement (Heckman & Enoka, 2012). A motor unit is defined as the motoneuron and the muscle fibers that its axon innervates(Liddell & Sherrington, 1925). Because of the tight neuromuscular junctions between axon terminals and muscle fibers, there is one to one relationship between action potentials in the motoneuron and motor unit firing patterns observed via electromyography (EMG) (Buchthal & Schmalbruch, 1980). Each motoneuron innervates a large number of muscle fibers and as a result, the individual waveform of muscle fibers reflects an amplified version of the discharge pattern of the parent motoneuron. These unique characteristics of motor units make the spinal motoneurons the only cells in the central nervous system (CNS) whose individual firing patterns can be routinely observed in intact humans. In fact, the first published data on motor unit discharge during voluntary contractions in humans date all the way back to 1920's (Wachholder, 1928). However, it is usually Adrian and Bronk who are credited to be the first to record unitary recordings of single motor units in humans (Adrian & Bronk, 1929). They used intramuscular electrode, which they called a concentric needle electrode, to record activities in the triceps muscle. In 1960's, John Basmajian improved the technique to record single motor unit activities and introduced the fine-wire electrodes, which are made from a pair of nylon-insulated, Karma alloy wires and are inserted into the muscle with a hypodermic needle (BASMAJIAN & STECKO, 1963). The ends of the wires were barbed so they would remain in the muscle when the needle was withdrawn. Compared to concentric needle electrode, the new

technique minimized pain and displacement of the electrodes during muscle contractions. However, fine-wire electrodes could only record a handful number of concurrently active motor units.

Although Hans Piper first attempted to record surface EMG signals in humans using a string galvanometer in 1912 (Piper, 1912), it wasn't until almost 100 years later that people tried to decompose surface EMG signals into firing patterns of individual motor units (De Luca, Adam, Wotiz, Gilmore, & Nawab, 2006; Farina, Arendt-Nielsen, Merletti, & Graven-Nielsen, 2002). The development of new electrodes and decomposition methods allowed non-invasive recordings of many concurrently firing motor units simultaneously. The latest technology using 64-channel high density surface array electrodes and convolutive blind source separation algorithm can decompose several tens of concurrently active motor units at the same time (Holobar, Minetto, Botter, Negro, & Farina, 2010; Nawab, Chang, & De Luca, 2010; Negro, Muceli, Castronovo, Holobar, & Farina, 2016).

Types of Motor Units

In 1973, Burke and Tsairis developed a scheme to classify motor units into three different categories based on physiological properties and histochemical profiles: slow (S), fast fatigue resistant (FR), and fast fatigable (FF) (Burke & Tsairis, 1973). They also differ in sizes that Type S motor units are the smallest and Type FF are the largest while Type FR in between the two. It was later shown that inputs to smaller motoneurons (i.e., motoneurons that innervate type S motor units) generate much higher excitatory postsynaptic potentials (EPSPs) and Ia EPSP amplitude was scaled with motor unit types (Henneman & Mendell, 1981). On the other hand, EPSPs from stimulation of the sural cutaneous nerve and the red nucleus were shown to

follow the opposite trend. However, one problem with the PSPs approach is that their amplitudes were not only dependent on underlying synaptic currents, but also their resistance. Therefore, even if Ia synaptic currents were equal in all motoneuron types, Ia EPSPs would be much higher in small motoneurons because of their high resistance. After separating these two factors, it was shown that Ia synaptic currents had a bias towards the smaller motoneurons (Heckman & Binder, 1988). Other descending inputs such as vestibulospinal, corticospinal, and rubrospinal were also unequal in the currents they generate with biases towards larger motoneurons (Powers & Binder, 2001). However, inhibitory inputs from Ia reciprocal inhibition and Rensahaw cells had approximately equal distribution on all motor types (Heckman & Binder, 1991; Lindsay & Binder, 1991). Simulation studies showed muscles with narrow recruitment ranges are likely to be primarily driven by descending inputs with small contributions from Ia afferent inputs (Heckman & Binder, 1993). Learning about these differences were important for understanding motor unit recruitment patterns in humans.

Motor Unit Recruitment and Rate Coding

Adrian and Bronk first observed that increases in force generation were achieved by the recruitment of additional motor units and an increase in the firing rates of already recruited units (Adrian & Bronk, 1929). In 1938, Denny-Brown and Pennybacker reported the fixed order of motor unit recruitment during a particular voluntary movement and called it "orderly recruitment" (Denny-Brown & Pennybacker, 1938). Finally, in 1965, Henneman and others published a seminal paper on the relationship between motor unit properties and motoneuron recruitment properties and summarized it to be called the "size principle" (HENNEMAN, SOMJEN, & CARPENTER, 1965). He stated "The amount of excitatory input required to

discharge a motoneuron, the energy it transmits as impulses, the number of fibers it supplies,

the contractile properties of the motor unit it innervates, its mean rate of firing and even its

rate of protein synthesis are all closely correlated with its size. This set of experimental facts

and interrelations has been called the 'size principle'." However, when people tried to observe

the size principle in humans using intramuscular needles, it met with some criticisms. Basmajian

argued that under certain conditions, humans could train to use visual and audio feedback of

motor unit firing to alter the recruitment order. In addition, Ashworth, Grimby and Hannerz

echoed Basmajian's argument that they observed reversals of recruitment order during slow

contractions (Ashworth, Grimby, & Kugelberg, 1967; Grimby & Hannerz, 1968, 1970). In 1972

and 1973, more people found concrete evidence of the size principle in human motor units in

the first dorsal interosseous muscle of the hand during voluntary isometric contractions

(Milner-Brown, Stein, & Yemm, 1972, 1973). Mendell and Henneman developed a new

technique that involved extracting the mechanical contribution of a motor unit to the force

generated by the whole muscle with the spike-triggered averaging method (Mendell &

Henneman, 1968, 1971). Stein and colleagues utilized this method to find a strong linear

correlation coefficient between the force of a motor unit and its recruitment threshold (Milner-

Brown et al., 1973). They concluded that human motor units were recruited in an orderly

sequence during ramp contractions.

Rate coding refers to motor units' strategy to increase discharge rates of already

recruited units in order to generate more force. Bigland and Lippold were the first to

characterize the relationship between mean discharge rate of motor units and muscle force.

They recorded motor units from the abductor digiti minimi brevis and observed that units

active at low tensions usually started firing at a much lower frequency and showed a greater

frequency range than those active at higher tensions (BIGLAND & LIPPOLD, 1954a, 1954b). They

stated that the relation between discharge rate and muscle force could be characterized with a

sigmoidal function and force gradation was largely explained by motor unit recruitment, except

at low and high contraction forces. Over the course of next 20 years, a couple of studies found

similar results in other muscles(Bracchi, Decandia, & Gualtierotti, 1966; Gydikov & Kosarov,

1974). However, it wasn't until 1977 that Monster and Chan published the seminal study on the

influence of rate coding on muscle force. They recorded ~500 individual motor units from the

extensor digitorum communis muscles from 8 men during slow voluntary isometric

contractions and showed that the minimal discharge frequency was similar for all unit at

around 8 to 16-24 Hz (Monster & Chan, 1977). Two years later, Kanosue and colleagues

recorded units from the brachioradialis muscle from 3 subjects and published a study that saw

a sigmoidal function with discharge rate and muscle force, similar to what Bigland and Lipplod

previously reported (Kanosue, Yoshida, Akazawa, & Fujii, 1979). Notably, they observed high-

threshold units reaching over 50 Hz in discharge rate during 75-100% maximum voluntary

contractions (MVC). They attributed the differences in findings to difference in muscle sizes and

suggested that rate coding might be the major mechanism for small muscles to control force,

whereas motor unit recruitment might be more important for large muscles.

Motor Unit Rate Modulation and Persistent Inward Currents

It was Schwindt and Crill who were the first to study PICs in motoneurons and

established that PICs could generate bistable behavior, which is defined as the continuous firing

of action potentials even after the input to the cell is ceased (Hounsgaard, Hultborn, Jespersen,

& Kiehn, 1984; Hounsgaard, Hultborn, et al., 1988; Hounsgaard & Kiehn, 1985, 1993;

Hounsgaard, Kiehn, & Mintz, 1988; P. Schwindt & Crill, 1977; P. C. Schwindt & Crill, 1981).

Shortly after, Hounsgaard and others discovered that PIC-induced bistable behavior was

mediated by monoamines such as serotonin (5HT) and norepinephrine (NE) from the brainstem

(Hounsgaard et al., 1984; Hounsgaard, Hultborn, et al., 1988; Hounsgaard & Kiehn, 1985, 1993;

Hounsgaard, Kiehn, et al., 1988). When descending monoaminergic tracts were blocked or

reduced through deep anesthesia or acute spinal transection, PIC amplitudes were greatly

reduced (Hounsgaard, Hultborn, et al., 1988; Miller, Paul, Lee, Rymer, & Heckman, 1996).

Without the monoaminergic input, motoneurons responded linearly to synaptic input. With

moderate level of neuromodulation, the input was amplified and motoneurons fired at a much

higher frequency. With high level of neuromodulation, the amplification was even greater and

self-sustained bistable behavior was reach. During the triangular input, two more important PIC

characteristics were revealed. The first was that once the initial acceleration phase was over,

the cell became much less sensitive to additional excitatory input and further increase in firing

rate was limited (i.e., rate saturation). The second characteristic was due to prolongation; the

offset of motoneuron firing was at a lower input level than the onset, resulting in onset-offset

hysteresis. Therefore, PICs induced three distinct phenomena in firing patterns: initial

acceleration, rate saturation, and hysteresis. These features of PICs have been observed in

various animal preparations including cats (Bennett, Li, Harvey, & Gorassini, 2001; Lee &

Heckman, 1998a), rats (Button, Gardiner, Marqueste, & Gardiner, 2006; X. Li et al., 2007; Y. Li et

al., 2004; Turkin, O'Neill, Jung, Iarkov, & Hamm, 2010), and mice (Meehan, Sukiasyan, Zhang,

Nielsen, & Hultborn, 2010).

In order to investigate the motoneuron outputs in response to descending inputs from the cortex, traditionally, currents were directly injected into spinal motoneurons and motor outputs were measured intracellularly. In anesthetized cats, when currents were injected in a slowly rising and falling manner (i.e., triangular injection), motor units modulated their firing frequencies linearly (Kernell, 2006). On the other hand in decerebrate preparations, a number of studies have shown the change in motor unit firing rates did not follow linearly with the trajectory of the slow ramp (Heckmann, Gorassini, & Bennett, 2005; Hounsgaard, Hultborn, Jespersen, & Kiehn, 1988; Lee & Heckman, 1998a, 1998b). At the point of recruitment, motor units increased their firing rates at a much sharper rate than the injected current. Before the point of inflection of the injected current, however, they reached a point where the degree in which firing rates increased drastically dropped and started to mirror the shape of the ramp more accurately. This phenomenon was referred to as rate limiting or rate saturation and had been demonstrated in many studies(De Luca & Contessa, 2012; De Luca, LeFever, McCue, & Xenakis, 1982; Fuglevand, Lester, & Johns, 2015; Gydikov, Kosarov, Tankov, & Shapkov, 1973; Monster & Chan, 1977). Later, studies have found that persistent inward currents (PICs) were mainly responsible for the mechanism of rate saturation (Heckmann et al., 2005).

In general, motoneuron PICs are made up of 50% NaPIC and 50% CaPIC (Y. Li & Bennett, 2003; Y. Li, Gorassini, & Bennett, 2004). The NaPIC is thought to be fundamental for spike initiation (Shapiro et al., 2001) while CaPIC is responsible for plateau potentials that induce self-sustained firing. CaPIC tends to fire continuously even when the activating input stops and produces "tail" current which is generated by L-type channels (Powers & Binder, 2001). NaPIC and CaPIC are both strongly facilitated by 5HT via 5HT2 receptors and by NE via α-1 receptors

(Harvey, Li, Li, & Bennett, 2006a, 2006b; Lee & Heckman, 1999; X. Li, Murray, Harvey, Ballou, & Bennett, 2007; Perrier & Hounsgaard, 2003).

When PICs were activated at a much lower input level with synaptic excitation than with injected currents which suggests that PICs were originated from dendrites (Bennett, Li, & Siu, 2001; Hultborn, Brownstone, Toth, & Gossard, 2004; Lee & Heckman, 2000). Therefore, PICs acted to amplify excitatory input once the activation threshold was reached. Current and voltage clamp studies have demonstrated that synaptic excitatory input could be amplified as much as fivefold and contributed to the gain control mechanism of the motor control system (Binder, 2003; Heckman, Lee, & Brownstone, 2003; Heckmann et al., 2005; Hultborn, 2002).

PIC estimation in humans

The hysteresis in motoneuron firing patterns has shown to be the most consistent phenomenon that could be used to estimate PICs in humans. The delta-F (ΔF) technique, which is a pairwise comparison method that measures hysteresis in a higher threshold unit in terms of lower threshold unit was first proposed by Gorassini and colleagues (M. Gorassini, Yang, Siu, & Bennett, 2002). The rationale was after the initial acceleration phase, the firing pattern of a lower threshold unit clearly mimicked the shape of current inputs to the motoneuron pool. Although the technique is more frequently used in human studies now, the inspiration for using firing rate of control unit as an estimate of the synaptic input to both units came from animal studies. Bennett and colleagues intracellularly injected slow triangular current ramps to sacro-caudal tail motoneurons of acute and chronic spinal rats in vitro. The intracellular recordings showed that after a motor unit was recruited and plateau potential was activated, its firing rate changed linearly, reflecting the shape of current injection (Bennett, Li, & Siu, 2001). While the

current was being injected, motor units were recorded from the same muscle simultaneously and ΔF method was invented to estimate PICs (Bennett, Li, Harvey, et al., 2001).

Animal studies have shown the importance of monoamines, which strongly facilitate PICs, in motor control (Kiehn, Erdal, Eken, & Bruhn, 1996; Steeves & Jordan, 1980). However, it was impossible to measure the magnitude of PICs in humans because researchers were unable to intracellularly record motoneuron activities. Gorassini and colleagues applied the ΔF method to successfully estimate the actual contribution of PICs in human soleus and the tibialis anterior (TA) muscles using fine-wire electrodes (M. Gorassini et al., 2002). Since then, others have used the intramuscular EMG and ΔF techniques to estimate PICs in healthy humans from various muscles (TA: (Stephenson & Maluf, 2011); Biceps and triceps: (Wilson, Thompson, Miller, & Heckman, 2015); Soleus: (Foley & Kalmar, 2019). ΔF was also measured in not only healthy, but also in abnormal conditions (Spinal cord injury: (M. A. Gorassini, Knash, Harvey, Bennett, & Yang, 2004; Mottram, Suresh, Heckman, Gorassini, & Rymer, 2009); Stroke: (Mottram et al., 2009).

The traditional intramuscular EMG could reliably measure the firing patterns of individual motor units. However, it was invasive in nature and also measured only a handful number of motor units at a time (Duchateau & Enoka, 2011). To overcome these limitations, researchers started employing non-invasive surface EMG electrodes and decomposition algorithms to capture the activities of a larger number of motor units. The first chapter of this thesis used 64-channel high density surface array electrodes and blind source separation algorithm to record and decompose activities of tens of motor units per contraction (Kim, Wilson, Thompson, & Heckman, 2020). In addition, two-source validation methods were

implemented to ensure the accuracy of surface array EMG decomposition. Spike by spike

comparison of motor units recorded simultaneously from intramuscular and surface array

electrodes showed the correspondence between the two methods was close to 90% or higher

(Kim et al., 2020; Thompson et al., 2018).

ΔF is currently the only method that is accepted as a standard to estimate PICs in

humans and some studies have shown that researchers should take few factors into

consideration when using ΔF. A simulation study of a simplified motor pool showed that other

than PICs, ΔF might be influenced by other intrinsic properties of motoneurons such as spike-

threshold accommodation and spike-frequency adaptation (Revill & Fuglevand, 2011). An

intramuscular EMG study of human soleus also showed that the speed of muscle contraction

can also alter ΔF measures (Vandenberk & Kalmar, 2014). The second chapter of the thesis

explored the effects of spike-threshold accommodation on ΔF by varying muscle contraction

speeds. Other than these intrinsic properties of motoneurons, other factors could also

influence ΔF values. A systematic study of various criteria for pairwise comparison from human

biceps showed that unit pairs with less than 1s time difference exhibit significantly lower ΔF

values (Hassan et al., 2020). Recent data from our lab also showed that excluding unit pairs with

less than 500 ms recruitment time difference increased ΔF values (Kim et al., 2020). A

continuous effort to improve and optimize the effectiveness of ΔF method should be made.

Goals for This Thesis

The overarching goal of this thesis is to examine PICs in humans and their role in human

motor control using the latest technology. The first chapter is titled "Differences in estimated

persistent inward currents between ankle flexors and extensors in humans." It establishes the

validity of studying PICs in humans using high-density surface array electrodes in sitting and

standing positions. Meanwhile, it compares ΔF in the tibialis anterior (TA) and the soleus

muscles to examine the difference in PICs between muscles with different functions. The

second chapter is titled "Muscle contraction speeds and their effects on persistent inward

currents in human ankle flexors and extensors." It further investigates ΔF in the TA and soleus

muscles and how they are affected by muscle contraction speeds. The last chapter is titled

"Properties of motor units of elbow and ankle muscles decomposed using high-density surface

EMG." It elucidates some of the strengths of high-density surface electrodes as well as some

potential limitations.

CHAPTER I. **Differences in estimated persistent inward currents between ankle flexors and extensors in humans**

Abstract

Persistent inward currents (PICs) are responsible for amplifying motoneuronal synaptic inputs and contribute to generating normal motoneuron activation. Delta-F (ΔF) is a well-established method which estimates PICs in humans indirectly from firing patterns of individual motor units. Traditionally, motor unit firing patterns are obtained by manually decomposing electromyography (EMG) signals recorded through intramuscular electrodes (iEMG). A previous iEMG study has shown that in humans, the elbow extensors have higher ΔF than the elbow flexors. In this study, EMG signals were collected from the ankle extensors and flexors using high-density surface array electrodes during isometric sitting and standing at 10% – 30% maximum voluntary contraction. The signals were then decomposed into individual motor unit firings. We hypothesized that comparable to the upper limb, the lower limb extensor muscles (soleus) would have higher ΔF than the lower limb flexor muscles (tibialis anterior, TA). Contrary to our expectations, ΔF was higher in the TA than the soleus during sitting and standing despite the difference in cohort of participants and body positions. The TA also had significantly higher maximum discharge rate than the soleus while there was no difference in rate increase. When only the unit pairs with similar maximum discharge rates were compared, ΔF was still higher in the TA than the soleus. Future studies will focus on investigating the functional significance of the findings.

Introduction

All motor commands act through motoneurons to activate muscles. Studies in animal

preparations, however, have shown that the electrical properties of motoneurons are complex.

For example, voltage-dependent persistent inward currents (PICs) allow spinal motoneurons to

continuously discharge action potentials even after the input to the cell ceases (Powers and

Binder 2001; Eken et al. 1989). Moreover, PICs are capable of amplifying motoneuronal

synaptic inputs three- to five-fold (Lee and Heckman 2000; Prather et al. 2001; Binder et al.

2002) and it is hypothesized that PICs play a role in maintaining postural muscle activation

(Brownstone 2006; Heckman et al. 2009; Johnson and Heckman, 2010).

PICs are strongly facilitated by monoamines such as serotonin (5HT) and norepinephrine (NE),

which are released by axons originating in the brainstem (Hounsgaard et al. 1988; Lee and

Heckman, 1999). Kiehn and Eken showed that selective depletion of 5HT and NE in the lumbar

spinal cord of rats induce postural deficits (Kiehn et al. 1996). Cats with monoamine depletion

also have severe deficits in posture and balance, despite unaffected stepping and locomotion

(Steeves and Jordan, 1980). Considerable evidence demonstrates the importance of PICs in

motor control and pathological motor behaviors, emphasizing the importance of studying the

functional role of PICs in humans (Gorassini et al. 2002a; Gorassini et al. 2002b; Gorassini et al.

2004). However, investigating the role of PICs in human motor control is challenging because it

is too invasive to directly measure the synaptic inputs of human spinal motoneurons.

In order to record the discharge of human spinal motoneurons, we exploited their key property,

which is a 1-to-1 ratio between the discharge rate of a motoneuron and the activation of

muscle fibers that it innervates (Buchthal and Schmalbruch 1980). Due to a large number of

muscle fibers innervated by each motoneuron, the individual waveform of muscle fibers

reflects an amplified version of the discharge pattern of the parent motoneuron. The

electromyography (EMG) signals from muscle fibers can be recorded using intramuscular

electrodes, making the spinal motoneurons the only cells in the CNS whose individual firing

patterns can be routinely measured in intact humans. A 64-channel high density surface array

electrodes (HD-sEMG) combined with automated decomposition algorithms can capture

several tens of concurrently active motor units (Holobar et al. 2010; Negro et al. 2016; Nawab

et al. 2010).

Gorassini and colleagues (Gorassini et al. 2002a; Gorassini et al. 1998; Gorassini et al. 2002b)

developed an indirect method to estimate the amplitudes of PICs in humans, termed delta-F

(ΔF). ΔF is calculated from pair-wise comparison of decomposed motor units from EMG signals

and it quantifies PIC activation during voluntary contractions (Gorassini et al. 2002a).

Previously, ΔF has been calculated in humans from EMG signals collected through fine-wire

intramuscular electrodes (iEMG) (Stephenson and Maluf, 2011; Wilson et al. 2015). However,

iEMG is not only invasive in nature but also can only capture EMG signals from a small number

of motor units per contraction (Duchateau and Enoka, 2011). This study attempted to apply the

non-invasive HD-sEMG technology to a well-established ΔF approach to estimate PIC

magnitude in humans. The extensive data provided by HD-sEMG have potential to study

motoneuron properties more in depth than iEMG (Collins et al. 2002; Farina and Negro 2015; Muceli et al. 2015).

PIC magnitude may not be equal between motor pools. For example, in cat motoneurons, plateau potentials of extensor motoneurons are more easily evoked than in the flexors (Hounsgaard et al. 1988). A recent study showed that the neck extensor motoneurons in cats have higher dendritic contacts from 5HT and NE boutons than the flexor motoneurons (Maratta et al. 2015). Consistent with findings in cat motoneurons, we have shown that, in the human upper limb, the elbow extensors have higher ΔF than the flexors (Wilson et al. 2015). The goal of this study was to establish the ankle flexor-extensor relationship in the human lower limb, using the latest motor unit decomposition technology. Characterized as ΔF, the magnitude of PICs during isometric force generation in the soleus and the tibialis anterior (TA) were measured in sitting and standing conditions. Because of the potentially important role of PICs in posture (Eken et al. 1989) and the greater PICs in extensors than flexors in the cat and human upper limb data, we hypothesized that the soleus would have higher ΔF than the TA in both sitting and standing positions.

Methods

Participants and Ethical Approval

A total of 23 young subjects with no history of neurological or motor disorders participated in the study. 12 subjects (aged 25 ± 3.6, 4 females) participated in the sitting down experiment and 11 subjects (aged 32.6 ± 14.4, 4 females) participated in the standing up experiment. All

procedures were performed in accordance with the Declaration of Helsinki and were approved

by the Institutional Review Board at Northwestern University. All subjects signed informed

consent form prior to participating in the study.

Experimental Procedures

Seated Experiment

Participants were asked to sit in a Biodex experimental chair (Biodex Medical Systems, Shirley,

NY) and secured with shoulder and thigh straps to minimize change in position. Each

participant's dominant foot (2 left, 10 foot) was attached to an ankle attachment, which was

anchored to Systems 2 Dynanometer (Biodex Medical Systems, Shirley, NY) to measure the

dorsi- and plantarflexion torque. Unless the participant expressed discomfort, the ankle was

positioned at 10° plantarflexion and the knee was positioned at 20° flexion. EMG signals were

recorded from the soleus and TA muscles. Before the surface arrays were applied, any excess

hair was removed, the skin was lightly abraded, and cleaned. After electrodes were applied,

each participant was asked to plantarflex and dorsiflex to their maximum effort in an isometric

condition up to three times. If one of the trials was less than 90% of the highest trial or the last

trial was clearly the highest, another maximum voluntary contraction (MVC) was performed.

MVC was calculated by taking the mean of three trials with the highest MVCs. Participants were

provided with a target line as well as live feedback of their torque (LabVIEW, National

Instruments, TX) and their task was to trace the target line with their torque feedback.

Depending on the trial, the peak of the target varied between 10% and 30% of each

participant's MVC. Prior to data collection, participants practiced until they were able to

smoothly trace the target line to the best of their abilities. During data collection, subjects

generated two identical ramps (10 second ascending and 10 second descending) per trial

interleaved with 10 seconds rest. Each trial was repeated up to 3 times and there were total of

12 trials (3 x 10% MVC dorsiflexion and plantar flexion each, 3 x 30% MVC dorsiflexion and

plantar flexion each). The trials were presented in a randomized order.

Standing Experiment

Participants were fitted into multiple degree of freedom (DOF), lower extremity isometric

device (the MultiLEIT, Sanchez et al. 2015) and secured with a harness and bracing. The foot of

the tested leg was casted and secured to two 6 DOF load cells to collect joint torque.

Participants were positioned to 10° hip abduction, 20° hip flexion, 25° knee flexion, and neutral

angle about the ankle. Before the surface arrays were applied, any excess hair was removed,

the skin was lightly abraded, and cleaned. EMG signals were collected from the soleus and TA

muscles. Each participant's MVC was measured during ankle plantarflexion and dorsiflexion and

real time visual feedback was provided (MATLAB, MathWorks, MA). Participants were asked to

reach their MVC as rapidly as possible and stay at the peak for at least one second. Participants

were then asked to generate 2 isometric ramp contractions (10 second ascending and 10

second descending) to 20% of their respective MVC. Each trial was repeated up to 3 times.

Data Collection

Surface EMG

Surface EMG recordings were collected through a 64-channel high-density surface array

electrode (HD-sEMG) from the soleus and the TA muscles. The array consisted of 64 (13 rows x

5 columns) gold-coated electrodes with 1 mm diameter and 8 mm inter-electrode distance

(ELSCH064NM2, OT Bioelettronica, Turin, IT). The location of the muscles was identified

through palpation before arrays were placed. The arrays were attached to the skin by bi-

adhesive foam (KITAD064, OT Bioelettronica, Turin, IT) and the skin to electrode contact was

optimized by filling the wells of the adhesive foam with conductive cream (CC1, OT

Bioelettronica, Turin, IT). The HD-sEMG signals were collected in differential mode, through one

of two amplifiers: a 12-bit A/D with x1,000 amplification (USB2, OT Bioelettronica, Turin, IT) or a

16-bit A/D with x150 amplification (Quattrocento, OT Bioelettronica, Turin, IT). Both amplifiers

filtered the signal at 10-900 Hz and digitized at a rate of 2048 Hz.

Intramuscular EMG

From 3 of the seated experiment participants, intramuscular EMG signals (iEMG) were collected

simultaneously with HD-sEMG signals. Up to three pairs of perpendicularly cut, bared, 75 μm

stainless-steel fine wires (Charlgren Enterprises, Gilroy, CA) were inserted into the soleus and

TA via a 23-gauge needle. HD-sEMG were placed over the wires for simultaneous EMG

collection between the two sources. iEMG signals are amplified (1-10k) and sampled at 10240

Hz (Quattrocento, 384-channel EMG amplifier, OT Bioelettronica, Turin, IT).

Motor Unit Decomposition

Surface EMG

Prior to decomposition, HD-sEMG signals were visually inspected and any channels with substantial artifacts or noise were removed. The remaining HD-sEMG data were decomposed based on convolutive blind source separation to provide motor unit spike train (Negro et al. 2016). The silhouette (similar to normalized measure of signal to noise ratio – see Negro et al. 2016) threshold for decomposition was 0.87.

Intramuscular EMG

iEMG signals were decomposed into individual motor units using the open source EMGLab software (McGill et al. 2005). During decomposition, signals were high-pass filtered (1000Hz) and a template matching algorithm automatically created templates, classified individual motor unit action potentials, and presented the residual signal. The remaining signals were manually inspected and decomposed to match either an existing template or into a new template. Spike times were then converted into instantaneous firing rates by calculating the reciprocal of the inter-spike interval.
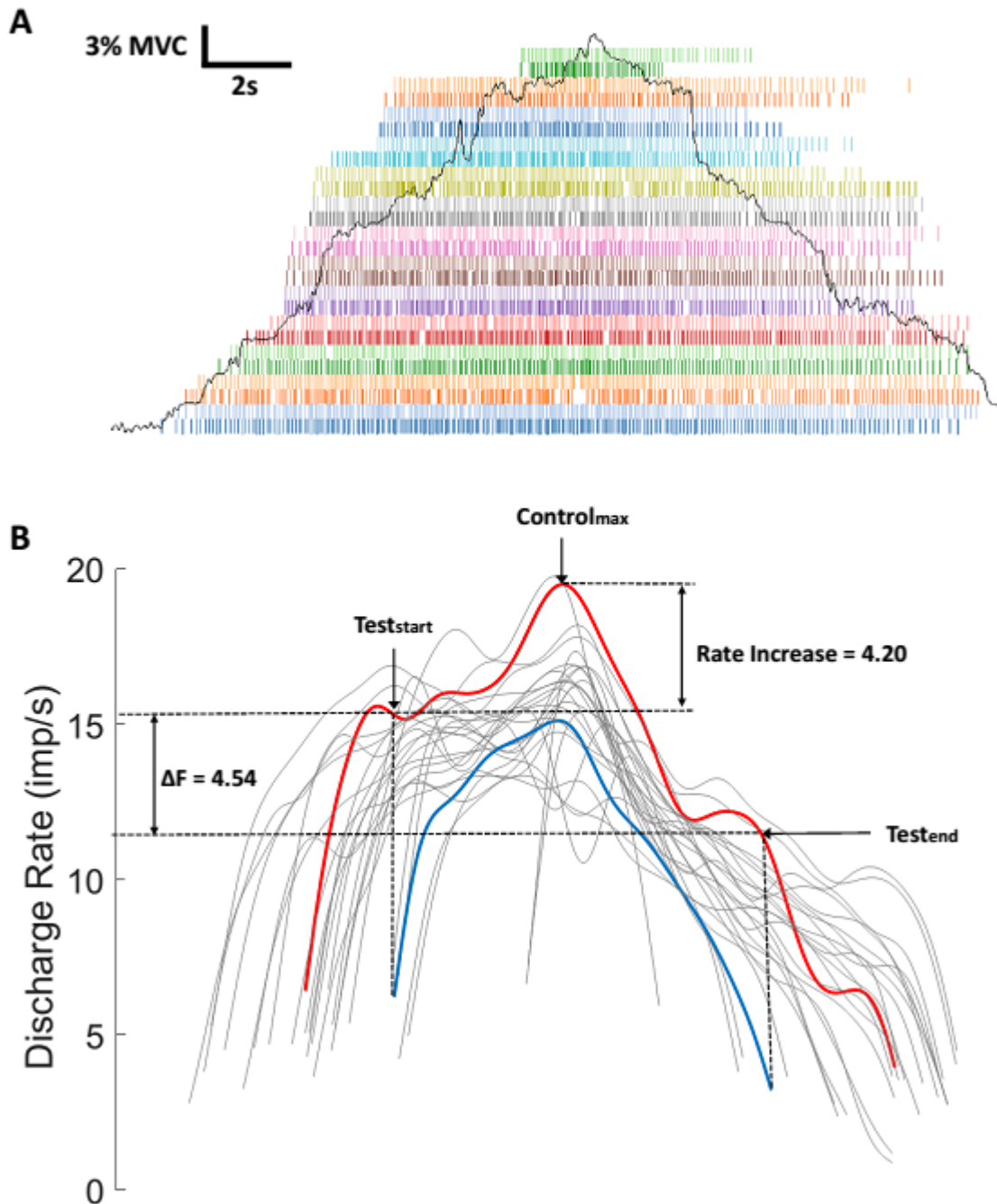
Figure 1. Pairwise comparison example. (A) Firing pattens of 26 motor units from the TA muscle during a single 30% MVC plantarflexion contraction. The ramp represents the torque trace produced by the participant and lasted for 20 seconds (10 second ascending and 10 second descending). (B) Discharge rates of 26 motor units after smoothed by 2-second hanning window. ΔF is calculated as the difference in discharge rate between the onset and offset of the test unit (blue) in terms of the control unit (red). Rate increase is the difference between the onset of test unit (Test$_{start}$) and the peak of control unit (Control$_{max}$).

Data Analysis

PIC estimation

A pairwise motor unit comparison technique, termed ΔF, was employed in this study to

indirectly estimate the level of PICs in motoneurons that innervate the soleus and the TA.

Figure 1B shows smoothed discharge rates of 26 motor units from the human TA in response to

a slow isometric ramp contraction. Units in red and blue illustrate ΔF calculation of pairwise

comparison. The earlier recruited unit is termed the control unit (red) and the later recruited

unit is termed the test unit (blue). The control unit was used as a reporter of changes in the net

excitatory synaptic input to the motoneuron pool and ΔF was calculated by taking the

frequency difference between the onset and the offset of the test unit in terms of the control

unit (Bennett et al. 2001; Gorassini et al. 1998). This paired motor unit analysis technique has

been used extensively (Herda et al. 2016; Mottram et al. 2009; Stephenson and Maluf 2011;

Udina et al. 2010; Wilson et al. 2015) and validated by experiments in animal preparations

(Powers et al. 2008).

Parameters to estimate PICs

The pairwise comparison technique assumes that the control and test units share common

synaptic drive and several studies have reported the coefficient of determination (r^2) as a

measure of common synaptic modulation between the two concurrently firing units (Gorassini

et al. 2004; Powers et al. 2008; Udina et al. 2010; Stephenson and Maluf 2011). Previous studies

have commonly used r^2 value of 0.5-0.7 as a threshold and in this study, any pairs with r^2 value

of less than 0.7 were excluded from data analysis (Wilson et al 2015; Foley and Kalmar 2019).

A simulation study has shown that there is a large variability in ΔF when the recruitment time difference between the test and control units is less than 500 ms (Powers and Heckman 2015). The high variability is possibly due to the initial acceleration phase of motor unit firing, which signifies activation of PICs (Johnson et al. 2017). Therefore, any unit pairs with a recruitment time difference less than 500 ms were excluded from analysis.

The rate-rate slope of each motor unit pair was also analyzed to gain understanding of the distribution of synaptic input to the motor unit pool (Gorassini et al. 2002a; Powers et al. 2012; Powers and Binder 2001; Johnson et al. 2017). The instantaneous firing rates of both motor units were first smoothed by 2-second hanning window. The rate-rate slope was then calculated by plotting firing rate of the test unit against the firing rate of the control unit during the descending phase of ramp contraction (Monster and Chan 1977). Higher the rate-rate slope, greater the tendency for synaptic inputs to be relatively larger in high than low threshold units (Johnson et al. 2017).

In order to ensure the difference in ΔF is not due to difference in firing rate ranges of motor units, a bootstrap technique was applied. We randomly selected 10 soleus unit pairs and compared their mean maximum discharge rates to mean maximum discharge rates of 10 randomly selected TA unit pairs. If the difference was within ± 0.02 imp/s, we noted their mean ΔF values. If the difference was bigger than ± 0.02 imp/s, we repeated the comparison up to 10000 times (each time is 10 randomly selected TA unit pairs). This was repeated 5000 times with replacement

Rate of Agreement

The rate of agreement (RoA) between HD-sEMG and iEMG decomposition was used as a

conservative estimate of accuracy and was defined by the following equation (Negro et al.

2016):

$$RoA = \frac{D_C}{D_C + D_A + D_W} 100\%$$

D_C represents the number of discharges common to the both sources within 0.5 ms of one

another. D_A represents the number of discharges identified only by HD-sEMG. D_W represents

the number of discharges identified only by iEMG. This approach treats each discharge equally,

without any bias toward either sources, and provides a normalized value, where 100% is a

perfect correspondence between HD-sEMG and iEMG.

Statistical Analysis

Values are reported as mean $\pm$ standard deviation (SD), unless otherwise noted. The mean ΔF

and rate increase were calculated in each muscle in each subject and then averaged across

subjects. Differences in the average ΔF and rate increase of each subject were evaluated by

using a mixed linear model with muscles as fixed effects and subject as a random effect. *Post*

hoc analyses were conducted with the Tukey honestly significant difference test. Statistical

significance was established at P < 0.05 and the Cohen's *d* was used to estimate the effect size

(ES) (Cohen, 1988).

Results

Motor Unit Yield

For the seated experiment, a total of 1259 (8.7 ± 3.0 per contraction) and 1699 (10 ± 6.5 per

contraction) motor units were collected from the soleus and the TA, respectively. From these

spike trains 10819 and 23121 motor unit pairs had r^2 values greater than 0.7. After eliminating

pairs with less than 500 ms recruitment time difference, 8443 soleus and 17987 TA motor unit

pairs remained for final analysis (Figure 2). For the standing experiment, a total of 756 (8.7 ± 5.3

per contraction) and 1395 (17.7 ± 6.8 per contraction) motor units were collected from the

soleus and TA. After controlling for r^2 values, 2379 soleus and 8637 TA motor unit pairs

remained, and 1749 soleus and 6486 TA motor unit pairs were included in the final analysis

after controlling for 500 ms recruitment time difference.

A
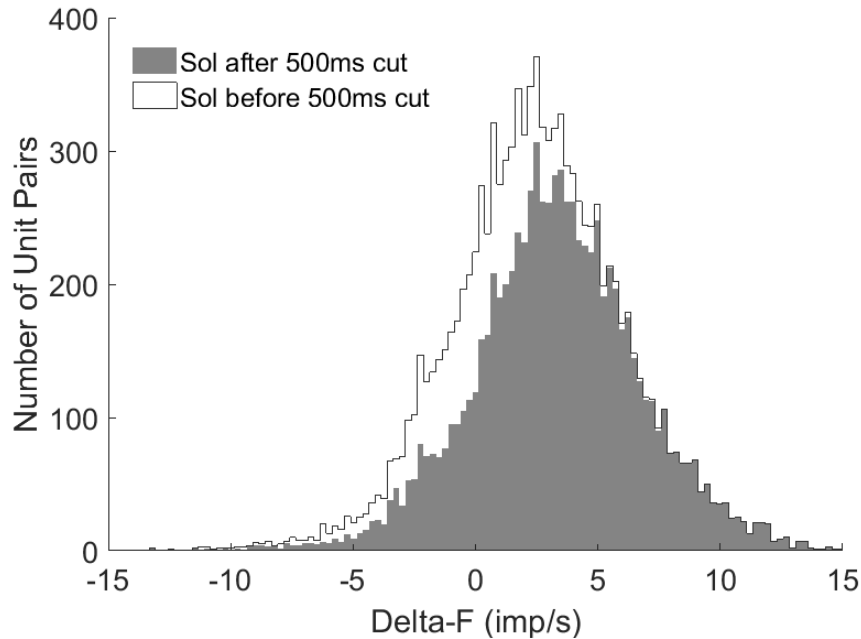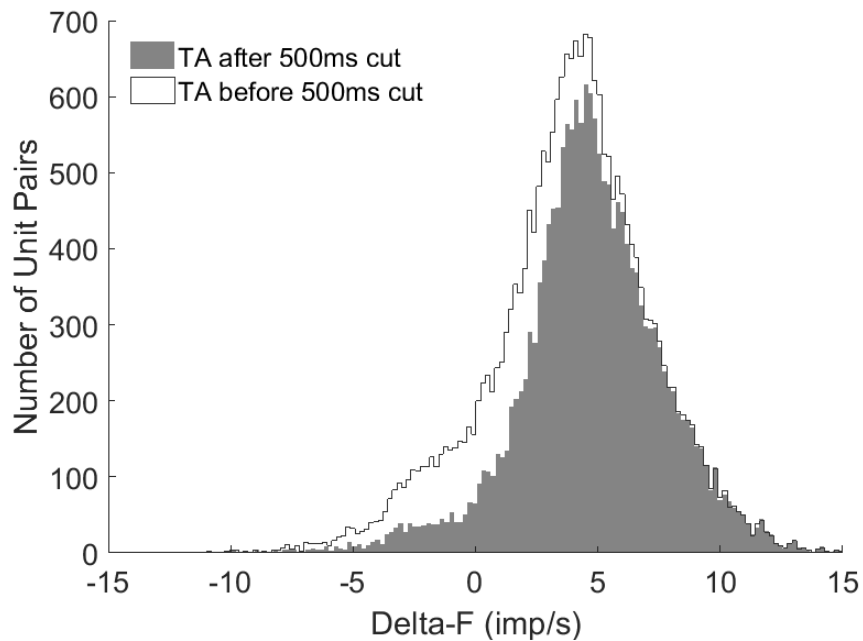
Figure 2. ΔF distribution before and after eliminating unit pairs with less than 500ms recruitment time difference. (A) Prior to controlling for the recruitment time difference, 10819 unit pairs were observed from the soleus. After making the 500ms recruitment time difference cut, 8443 unit pairs remained for analysis. (B) There were 23121 unit pairs observed from the TA before controlling for the recruitment time difference. After, 17987 unit pairs remained for analysis. For both muscles, eliminated unit pairs mostly had lower ΔF than remaining unit pairs. The Kolmogorov-Smirnov test verified that the ΔF distributions are not statistically different than normal (p < 0.0001).

Silhouette Values

During seated experiment, the soleus units had a mean silhouette values of 0.97 ± 0.0067 and

0.92 ± 0.0049 at 10% and 30% effort levels. The TA units had a mean silhouette values of 0.92 ±

0.0048 and 0.92 ± 0.0040 at 10% and 30% effort levels. During standing experiment, the soleus

had 0.93 ± 0.0049 and the TA had 0.93 ± 0.0030 silhouette values at 20% effort level.
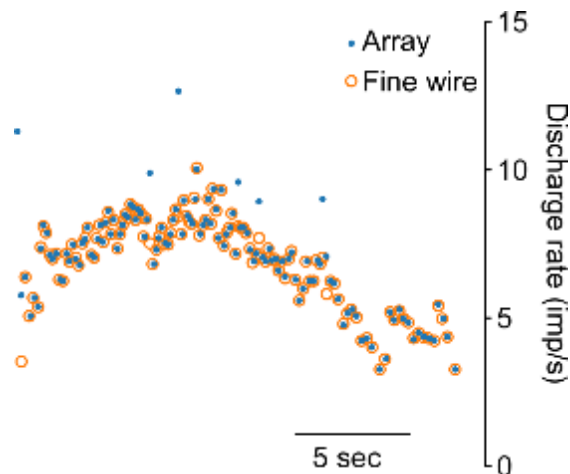
Figure 3. Example of a motor unit identified from both sources during a 10% MVC trial in the soleus. The RoA between iEMG and sEMG in this example is 93.9%.

Rate of Agreement

Through fine-wire recordings, total of 252 soleus (7 ± 5.6 units per trial) and 65 TA units (1.8 ±

1.3 units per trial) were collected during sitting isometric force generation. A total of 34 soleus

units were identified from both HD-sEMG and iEMG, whereas only 5 TA units were detected

from the both sources. Figure 3 represents a common motor unit to both iEMG and HD-sEMG

with RoA of 93.9%, during a single contraction in the soleus. On average, RoA between the two

sources was 86.0 ± 10.6% and 90.8 ± 4.5% for the soleus and TA, respectively.

Sitting Isometric Force Generation

Under 10% effort level, the soleus and the TA showed ∆F values of 3.06 ± 0.86 imp/s and 4.61 ± 1.15 imp/s and under 30% effort level, they were 3.65 ± 0.77 imp/s and 4.69 ± 0.62 imp/s, respectively. The results showed that during sitting isometric force generation, the TA exhibited significantly higher ∆F than the soleus in both 10% (p < 0.0001; ES = 1.53) and 30% (p = 0.0039; ES = 1.49) effort levels (Figure 4A). On the other hand, within muscles, there was no statistical significance in ∆F between 10% and 30% effort levels (Soleus p = 0.089; ES = 0.72; TA p = 0.82; ES = 0.087).
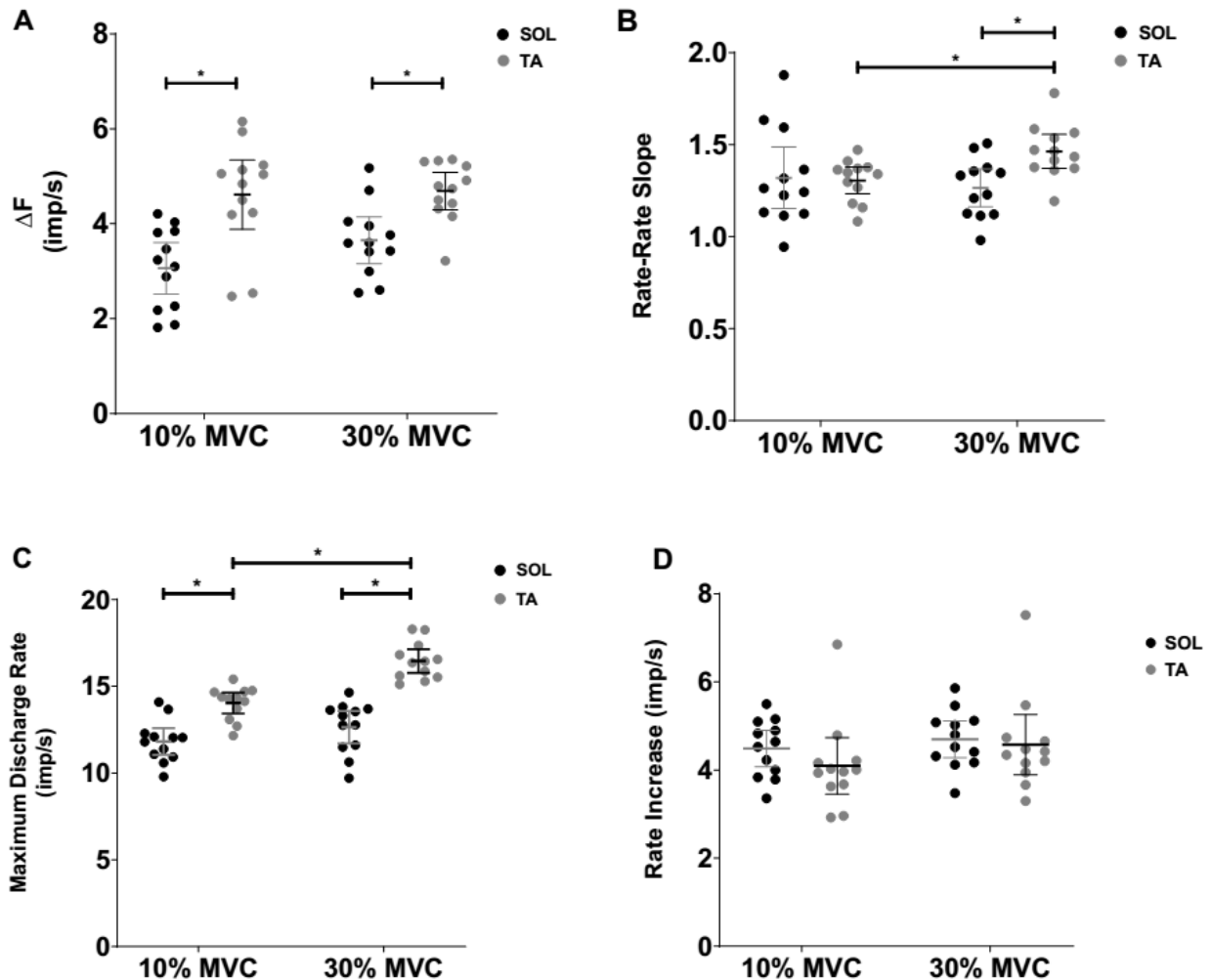
Figure 4. Mean (-) and 95% CI shown for sitting experiment. (A) ΔF was significantly higher in the TA than the soleus during 10% (p < 0.0001) and 30% (p < 0.0039) MVC conditions. Increasing the effort level did not change ΔF values in both muscles. From left to right, the mean ΔF values are 3.06 ± 0.86 imp/s, 4.61 ± 1.15 imp/s, 3.65 ± 0.77 imp/s, and 4.69 ± 0.62 imp/s. (B) The mean rate-rate slope of the soleus and TA at 10% MVC are 1.31 ± 0.26 and 1.32 ± 0.11 and at 30% MVC, they are 1.26 ± 0.16 and 1.46 ± 0.15. The rate-rate slope of the soleus does not change significantly between effort levels (p = 0.43) but the rate-rate slope of the TA does (p = 0.0254). Statistical difference was observed between the muscles at 30% MVC (p = 0.0056) but not at 10% MVC (p = 0.84). (C) The mean maximum discharge rate of the test units at 10% MVC are 11.82 ± 1.21 imp/s and 14.03 ± 0.95 imp/s and at 30% MVC, they are 12.64 ± 1.47 imp/s and 16.46 ± 1.07 imp/s. The maximum discharge rate of the soleus does not change significantly between effort levels (p = 0.063), while the statistical significance is observed in the TA (p < 0.0001). The maximum discharge rates between muscles are also significantly different at both effort levels (p < 0.0001). (D) Rate increase did not change significantly between conditions. From left to right, the values were 4.48 ± 0.65 imp/s, 4.09 ± 1.01 imp/s, 4.70 ± 0.66 imp/s, and 4.60 ± 1.10 imp/s.

Figure 4B shows the soleus rate-rate slope was 1.31 ± 0.26 at 10% effort level and when the effort level was increased to 30%, there was no significant change in the slope (1.26 ± 0.16) (p = 0.43; ES = 0.23). On the contrary, the TA rate-rate slope significantly increased from 1.32 ± 0.11 at 10% to 1.46 ± 0.15 at 30% effort level (p = 0.0254; ES = 1.064). There was no statistical difference between the rate-rate slope of the soleus and the TA at 10% effort level (p = 0.84; ES = 0.050), but the difference exceeded the threshold for statistical significance when the effort level was increased to 30% (p = 0.0056; ES = 1.29). These results were consistent with a previous study showing that rate-rate slopes are generally greater than 1.0 (Monster and Chan 1977; Bennett et al. 2001).

During sitting isometric force generation, the test units of the soleus had an average maximum discharge rates of 11.82 ± 1.21 imp/s at 10% and 12.64 ± 1.47 imp/s at 30% MVC. Despite slight increase in maximum discharge rates, there was no statistical significance between effort levels

(p = 0.063; ES = 0.61). The test units of the TA had an average maximum discharge rates of

14.03 ± 0.95 imp/s at 10% and 16.46 ± 1.07 imp/s at 30%. Unlike the soleus, there was a

statistical difference between effort levels in the TA (p < 0.0001; ES = 2.40). The maximum

discharge rates were statistically different between the muscles at both effort levels with large

effect sizes, with soleus tending to have lower rates (p < 0.0001 for soleus and TA; ES = 2.03 at

10%; ES = 2.97 at 30%) (Figure 4C). The results showed that the soleus rate increase values

were 4.48 ± 0.65 imp/s at 10% effort level and 4.09 ± 1.01 imp/s at 30% effort level. There was

no statistical difference between effort levels (p = 0.53; ES = 0.26). The TA rate increase values

were 4.70 ± 0.66 imp/s at 10% effort level and 4.60 ± 1.10 imp/s at 30% effort level. There was

no statistical difference between effort levels in TA either (p = 0.15; ES = 0.38). There was no

statistical differences between muscles either (p = 0.24; ES = 0.41 at 10% and p = 0.71; ES = 0.12

at 30% effort level).
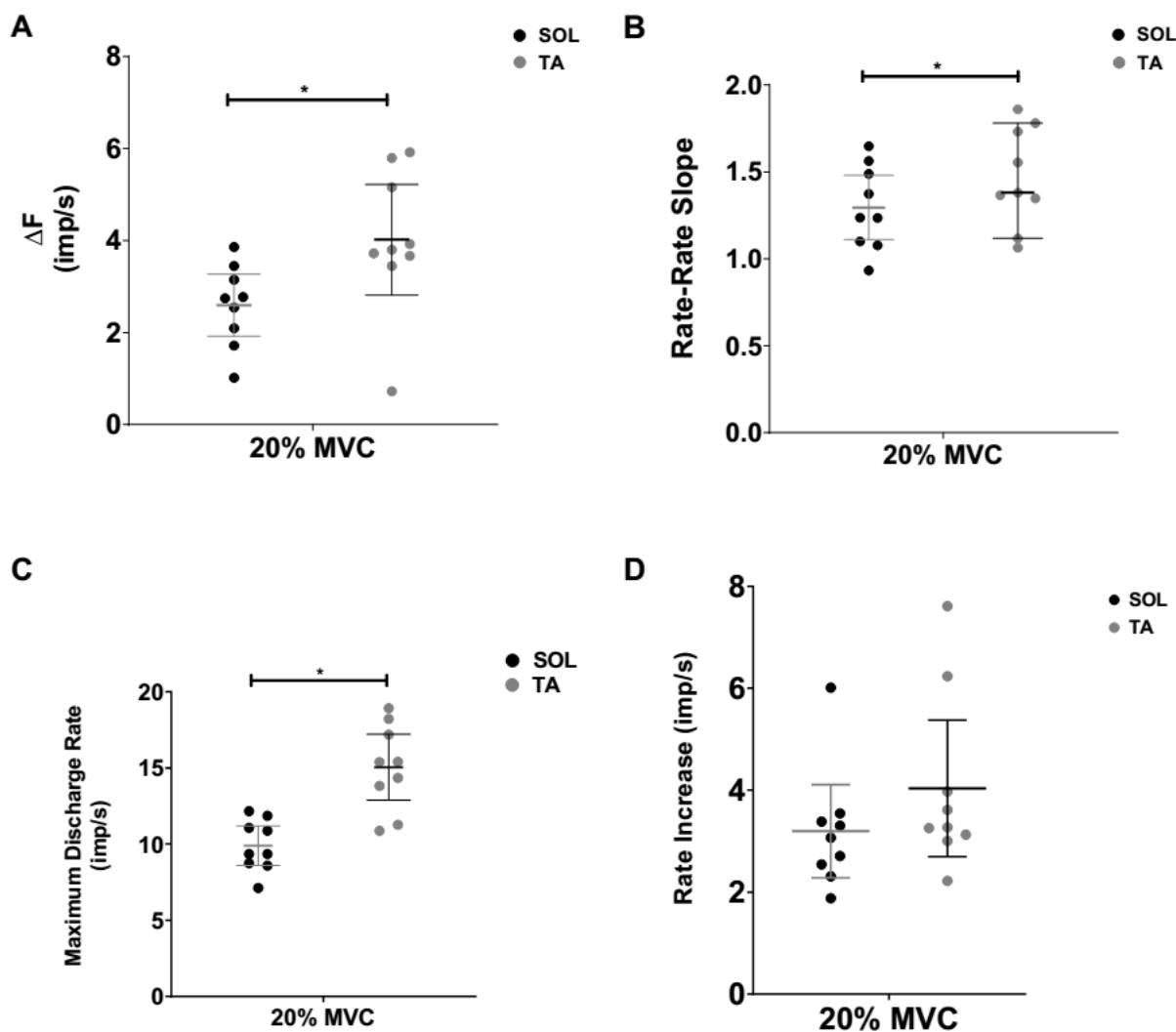
Figure 5. Mean (-) and 95% CI shown for standing experiment. (A) At 20% MVC, the mean ΔF of the soleus was 2.59 $\pm$ 0.88 imp/s and the TA was 4.02 $\pm$ 1.56 imp/s and there was a statistical significance between them (p = 0.022). (B) At 20% MVC, the mean rate-rate slope of the soleus and the TA were 1.30 $\pm$ 0.24 and 1.47 $\pm$ 0.28 and they were statistically different (p = 0.0042). (C) At 20% MVC, the mean maximum discharge rates of the test units were 9.90 $\pm$ 1.69 imp/s for the soleus and 15.05 $\pm$ 2.82 imp/s for the TA and they were statistically different (p < 0.0001). (D) The mean rate increase did not show statistical difference between muscles. Their values were 3.19 $\pm$ 1.19 imp/s for the soleus and 4.04 $\pm$ 1.74 imp/s for the TA (p = 0.44).

Standing Isometric Force Generation

Figure 5A shows that during standing isometric force generation at 20% MVC, the TA (ΔF = 4.02 $\pm$ 1.56 imp/s) exhibited significantly higher ΔF than the soleus (ΔF = 2.59 $\pm$ 0.88 imp/s) (p =

0.022; ES = 1.13). Figure 5B shows that the TA rate-rate slope during standing (1.47 ± 0.28) was

significantly higher than the rate-rate slope of the soleus (1.30 ± 0.24) (p = 0.0042; ES = 0.65).

As shown in Figure 5C, the soleus and the TA test units had mean maximum discharge rates of

9.90 ± 1.69 imp/s and 15.05 ± 2.82 imp/s, with statistical significance between them (p <

0.0001; ES = 2.22). Figure 5D shows the rate increase in the soleus was 3.19 ± 1.19 imp/s and in

the TA was 4.04 ± 1.74 imp/s. No statistical significance was observed between the muscles (p =
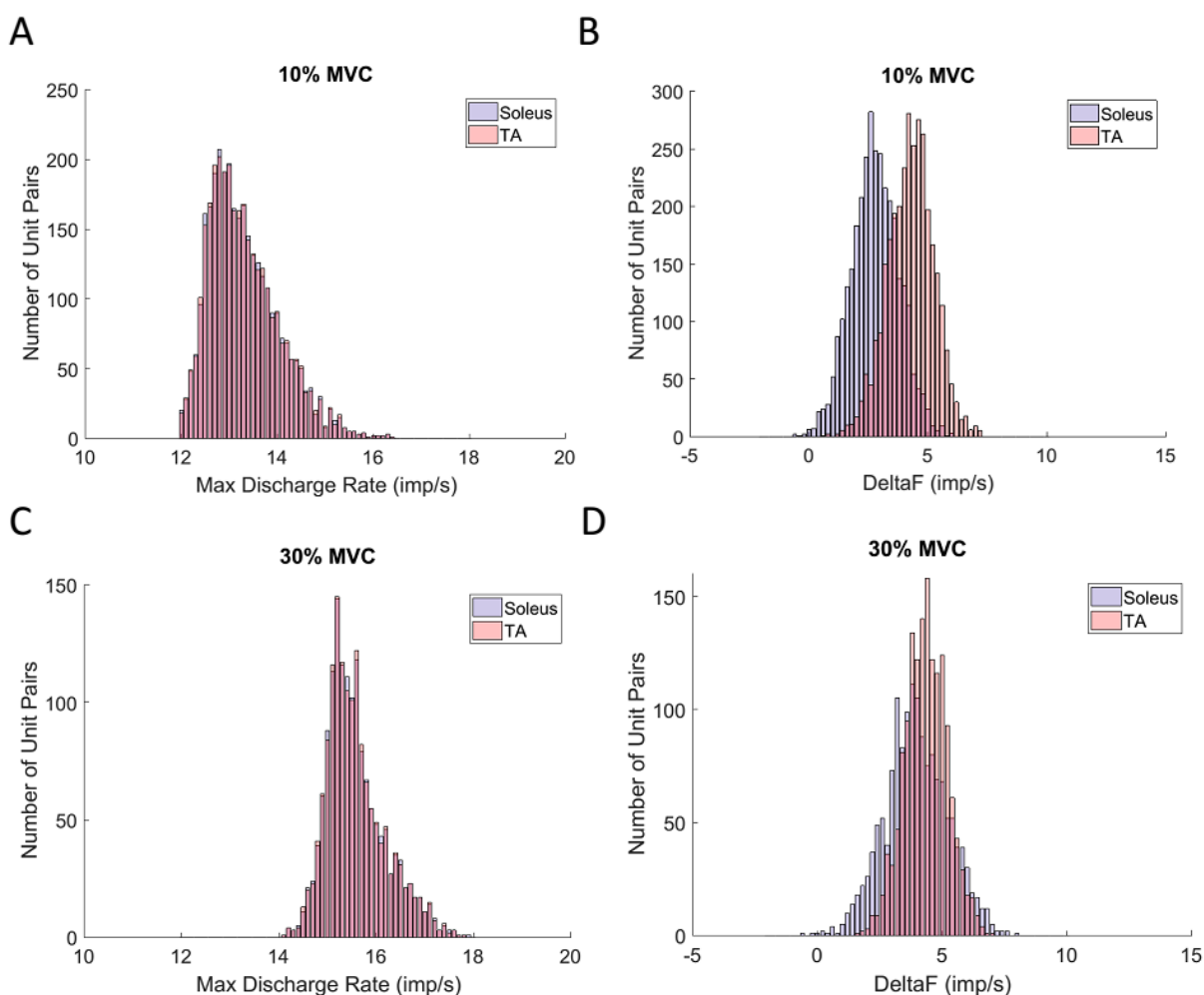
0.44; ES = 0.56).

Figure 6. ΔF after matching maximum discharge rates. (A) Under 10% MVC condition, there
was no statistical difference between the maximum discharge rates of the matched soleus
(13.35 ± 0.75 imp/s) and TA (13.35 ± 0.75 imp/s) unit pairs (p = 0.50). (B) The matched ΔF
values of the soleus (2.87 ± 1.00 imp/s) and TA (4.38 ± 0.97 imp/s) units had significantly

different (p < 0.00001). (C) There was no statistical difference (p = 0.33) in maximum discharge rates between the muscles under 30% MVC condition (soleus = 15.64 ± 0.62; TA = 15.64 ± 0.62). (D) Statistical significance was observed between the matched ΔF values of the soleus (4.06 ± 1.27) and TA (4.44 ± 0.84) (p < 0.00001).

Comparisons at Matched Firing Rates

The lack of difference in firing rate increase between soleus and TA indicates that the higher peak firing rate of TA was not the source of its higher delta ΔF amplitudes. To further investigate this issue, ΔF was compared between the muscles with the unit pairs that had similar maximum discharge rates in control units. After 5000 comparisons, 3196 (10% MVC sitting), 1524 (30% MVC sitting), and 40 (20% MVC standing) unit pairs had qualifying matching maximum discharge rates. As shown in Figure 6A and C, the unit pairs included in the analysis had almost identical mean maximum discharge rates between the soleus and TA (13.35 ± 0.75 imp/s for 10% effort level and 15.64 ± 0.62 imp/s for 30% effort level). However, in both effort levels, ΔF was still significantly higher (p < 0.00001) in the TA than the soleus (Figure 6B and D). Also, during standing, the mean maximum discharge rates of the unit pairs were almost identical (14.02 ± 0.38 imp/s) and ΔF was still significantly higher (p = 0.0037) in the TA (3.87 ± 0.82 imp/s) than the soleus (3.23 ± 0.85). These results for matching firing rates are consistent with the lack of difference in rate increase (Figs. 4D, 5D), making it unlikely that higher peak firing rates accounted for the larger values for ΔF in TA compared to soleus.

Discussion

The goal of this study was to estimate the contribution of PICs during isometric force generation and explore the flexor-extensor relationship in the ankle muscles. HD-sEMG signals

were recorded from young adults and the EMG signals were decomposed into discharge

patterns of individual motor units for pair-wise comparison. The results suggest that contrary to

our hypothesis, the TA has significantly higher ΔF values than the soleus.

ΔF indirectly measures PICs

In anesthetized cats, triangular current injection generates a relatively linear firing response in

motoneurons. However, in decerebrate cats when PICs are facilitated by tonic descending

monoaminergic drive, motoneurons respond in three distinct phases: initial acceleration,

saturation, and hysteresis (Powers and Binder 2001; Heckman and Enoka 2012). Because PIC

amplitude is directly proportional to the level of monoaminergic inputs, any of the three phases

can be used to estimate PICs (Johnson et al. 2017). Estimates of ΔF is however highly variable

when acceleration phase is included (Kim et al. 2017) and the saturation phase is sensitive to

the relative distribution of synaptic input on high versus low threshold motoneurons (Johnson

et al. 2017). We thus focused on the ΔF calculation to indirectly quantify hysteresis generated

by PICs (Kiehn and Eken 1997; Gorassini et al. 1998; Gorassini et al. 2002a; Gorassini et al.

2002b).

One of the assumptions of the ΔF calculation is that the motor unit pairs receive a common

synaptic input. In order for the control unit to act as a reporter of changes in the net excitatory

synaptic input to the motoneuron pool, the changes in discharge rate of the test unit should be

highly correlated with the changes in the control unit. Therefore, it is generally assumed that

the correlation coefficient r^2 value greater than 0.7 would adequately estimate the excitatory

net synaptic input to the motoneuron pool shared with the test unit (Gorassini et al. 2004; Powers et al. 2008; Udina et al. 2010; Stephenson and Maluf 2011).

Simulation of motor unit pairs has shown that when the control and test units have a recruitment time difference of less than 500 ms, there is a large variance in ΔF values (Powers and Heckman 2015). The initial acceleration phase of a motor unit discharge pattern indicates activation of the PIC and if the pair-wise comparison is computed before the acceleration phase of the control unit is terminated, it can cause a large variance in ΔF. For the same reason, unit pairs with less than 500 ms recruitment time difference generally have lower ΔF values because they were captured prematurely (i.e. before PICs were fully activated). As shown in figure 2, any unit pairs that did not meet the criterion were excluded from further analysis.

Two Source Validation

The most stringent method of validating motor unit decomposition is recording the same motor unit from two separate sources and to compare their discharge patterns (Mambrito and De Luca 1984). This method assumes that it is highly unlikely to identify a faulty motor unit from two separate methods of recording and decomposition. The RoA values observed in this study as well as the proportion of the matched units are similar to previously reported values (Yavuz et al. 2015). The lower number of matched units can be attributed to the bias of sEMG decomposition toward more superficial units (Holobar et al. 2009). In addition, it has been previously shown that as the contraction speed increases, the number of lower threshold unit

decomposed is decreased with sEMG (Hassan et al. 2019), which has not been reported in iEMG

yet.

Greater ΔF in the TA than the soleus

Our results showed that ΔF of the ankle dorsiflexors (i.e. TA) is larger than the ankle

plantarflexors (i.e. soleus), regardless of effort levels or body positions. These results were

surprising for two reasons. First, the findings of the current study were contradictory to

previous findings in the upper limb which showed that the extensor (i.e. triceps) had higher ΔF

than the flexors (i.e. biceps) (Wilson et al. 2015), a relationship that is consistent with previous

findings in decerebrate cat and neonatal rat preparations (Hounsgaard et al. 1998; Cotel et al.

2009). Surprisingly, our results showed that in the human lower limb, the flexor and extensor

relationship was reversed. Moreover, this "reversed" relationship continued to hold during

standing, a finding consistent with recent results showing that ΔF of soleus motor units remains

the same as a subject goes from sitting to standing (Foley and Kalmar 2019).

Second, the soleus exhibits tonic activation during postural control and PICs are important for

maintaining prolonged self-sustaining firing (Sinkjaer et al 2000; Hounsgaard et al. 1988). Our

findings were especially surprising because the prolonged firing would seem to be a major

advantage for maintenance of posture (Heckman and Johnson, 2014). During standing in

humans, the soleus is tonically active but TA is not (Day et al. 2013). Furthermore, during the

sitting/isometric condition of our experiment, reciprocal Ia inhibition is much stronger onto TA

than the soleus synergist, medial gastrocnemius (Yavuz et al. 2018). Reciprocal inhibition is

especially relevant because PICs are highly sensitive to this form of inhibition, with even small

increases in length of antagonists causing large reductions in PIC amplitudes (Hyngstrom et al.

2007). Thus, it is possible that L-type $Ca_V1.3$ channels or monoaminergic boutons are more

highly expressed in the TA than the soleus in humans. In addition, these results might also

suggest that TA motoneurons receive substantially stronger monoaminergic synaptic drive from

the brainstem, more so than soleus motoneurons. It is possible that ΔF values can be limited by

firing rate ranges of motor unit populations and it might partly explain why ΔF was lower in the

soleus than the TA. This possibility was explored by measuring rate increase, which is the

maximum possible ΔF of a motor unit pair minus actual ΔF (Figure 1B). As the rate increase

approaches zero, the possibility of limiting ΔF gets bigger due to saturation. However, our

results showed that there were large rate increases for every condition we measured, without

any significant difference between them.

It is also possible that higher ΔF in the TA than the soleus is due to difference in overall firing

rate ranges of the two motor unit populations. This difference however does not appear to

affect our measurements of ΔF in the two muscles. Our analysis of rate increase (which is the

increase in firing rate of the control unit from recruitment of the test unit to peak firing – see

Methods) was not different between TA and soleus (Figures 4D and 5D). In addition, we

compared ΔF values of motor unit pairs with similar maximum discharge rates (Figure 6). The

results showed that the TA still had significantly higher ΔF than the soleus under all conditions.

The difference between bipeds and quadrupeds

Although the difference between cat and human motoneurons is unexpected, it is not unwarranted. The muscle fiber composition of the soleus and the TA is a lot more similar in humans than cats (Johnson et al. 1973). Additionally, it has already been shown that cat and human ankle muscles respond differently to stimulation. For example, the spinal motoneurons of cats only show suppression during fictive locomotion (Perreault et al. 1999; Gosgnach et al. 2000; and Menard et al. 2003). However, in humans, during rhythmic arm movement, the TA h-reflex amplitude is modulated bidirectionally (suppression and facilitation), while the soleus only exhibits suppression (Dragert and Zehr 2009). It is possible that these differences are due to the fact that the ankle muscles of bipeds and quadrupeds serve different functional roles.

No change in ΔF between effort levels

Another surprising finding from this study was that during sitting isometric force generation, there was no statistical significance in ΔF between effort levels. A previous study has shown that with increasing background EMG, the H-reflex amplitude of the soleus increases (Capaday and Stein 1987; Edamura et al. 1991; Kido et al. 2004; Capaday and Stein 1986), and we expected to observe increase in ΔF as well due to increasing monoaminergic drive from the brainstem. Our results suggested that monoaminergic drive might stay approximately constant as the drive from other descending systems, such as the corticospinal tract, increase to produce more motor output. However, it is also possible that the difference in rates of rise (Revill and Fuglevand 2011) and/or activated motor unit populations between effort levels minimized the increased in ΔF.

Maximum discharge rates

Along with ΔF, the mean maximum discharge rate of the TA was significantly higher than the soleus under all conditions. Increasing effort level from 10% to 30% also significantly increased the mean maximum discharge rate of the TA and although statistical significance was not reached, the mean maximum discharge rate of the soleus also increased. As descending commands strengthen, muscles produce more output by recruiting more units and increasing discharge rates. It is possible TA relies more on the latter strategy while increasing force output from 10% to 30% effort level. It is also unlikely that the higher maximum discharge rate of TA affected ΔF measurements for two reasons. First, there was no difference in rate increase between the muscles. Second, even after motor unit pairs were normalized by their maximum discharge rates, ΔF was still significantly higher in the TA than the soleus.

The rate-rate slope and its sensitivity to changes in synaptic inputs

As shown in figure 4B, the soleus rate-rate slope did not significantly change between effort levels. However, as the effort level increased, the rate-rate slope of the TA slightly, but significantly, increased. Rate-rate slope measures two factors: the relative share of the synaptic input to the two units and the relative behaviors of their intrinsic frequency to current slopes (including PIC effects) (Gorassini et al. 2002a; Powers et al. 2012; Powers and Binder 2001). If both factors are equivalent, rate-rate slope will be equal to 1.0 (Johnson et al. 2017). A slope greater than 1.0 indicates that either the higher threshold unit is more sensitive to a given increment in drive, due to a higher frequency-current slope, or it receives more excitatory input than the lower threshold unit. A tendency to generate greater synaptic current in F vs S

motoneurons is a hallmark of several descending systems, including the corticospinal and

vestibulospinal inputs, whereas Ia input from the periphery has the opposite effect (Powers and

Binder 2001). Thus, a rate-rate slope greater than 1 may indicate a dominance of descending

inputs in the overall motor command for increasing volitional torque. Because of this slope

interact with intrinsic current slopes and PIC effects, it is however likely that spacing between

the recruitment thresholds of motoneurons is a better index of synaptic distribution (Heckman

et al. 1993; Johnson et al. 2017). We plan further analyses using this approach.

Conclusion

In this study, we estimated the contribution of PICs during sitting and standing using the latest

HD-sEMG technology. This study showed regardless of body position, the TA has higher ΔF than

the soleus during isometric force generation. These results indicated the motoneurons that

innervate TA receive more neuromodulatory inputs from the brainstem and generate stronger

PICs. These results were surprising because they were contradictory to the results shown in

human elbow and cat ankle muscles (Wilson et al. 2015; Hounsgaard et al. 1998). However, the

difference between motoneuron excitability in humans and cats has been previously reported

and therefore is not completely surprising (Perreault et al. 1999; Gosgnach et al. 2000; and

Menard et al. 2003; Dragert and Zehr 2009). Increased effort levels did not significantly change

ΔF values in either of the muscles, implying that monoaminergic drive stays relatively constant

as the descending drive from other systems such as corticospinal tract increases to produce

higher torque levels. Although statistical significance was not reached in the soleus, the

maximum discharge rate increased in both muscles as the effort level increased. It is possible

that the TA especially relies on increasing discharge rate to increase motor output from 10% to

30% effort level. The results after normalizing for the mean maximum discharge rate showed

that the difference in discharge rate range was not the cause of difference in ΔF between the

muscles. The rate-rate slopes were greater than 1 across all conditions, consistent with a

previous study (Monster and Chan 1977), suggesting a greater distribution of synaptic input

onto high versus low threshold units. In conclusion, the soleus and the TA exhibit substantial

magnitude of PICs, characterized as ΔF, during isometric force generation. Despite the findings

in the upper limb and the soleus' tonic EMG activity during postural control, the TA exhibits

significantly higher ΔF. Although the data were taken from two different cohort of participants,

the same trend was observed in both sitting and standing conditions. In the future, the

functional significance of the findings will be explored by directly comparing ΔF values during

sitting and standing from the same cohort of participants.

CHAPTER II. **Muscle contraction speeds and their effects on persistent inward currents in human ankle flexors and extensors**

Abstract

Persistent inward currents (PICs) are thought to be the most prominent intrinsic property of motoneurons that disrupt the simple synaptic input-output relationship in motor control. PICs enable the bistable behavior in motoneurons and are thought to play an important role in balance and postural control. A previous study used delta-F (ΔF) method to establish the level of PICs in humans during sitting and standing positions. Surprisingly, the results showed that varying effort level did not affect ΔF. However, the study compared ΔF values at different muscle contraction speeds which could have potentially confounded the results. In this study, we continued the effort to better understand PICs in humans and how ΔF is affected under different conditions. We recorded and decomposed motor unit activities from the soleus and tibialis anterior (TA) muscles of young and healthy adults. We analyzed ΔF values and other firing properties at 2 different % maximum voluntary contraction (MVC) levels (10% and 30% MVC) and 3 different muscle contraction speeds at each effort level (10% MVC - 1, 2, and 5%

MVC/s; 30% MVC – 3, 6, and 15% MVC/s). We also tracked motor units across different contraction speeds based on motor unit action potential profiles to observe how individual units were affected. The results showed that increasing speeds does not change ΔF or peak firing rates. However, initial and final firing rates were significantly increased as the muscle contraction speed increased. We concluded that faster muscle contraction speed did not require more monoaminergic inputs from the brainstem. However, it could be potentially achieved by more synaptic inputs from the cortex.

Introduction

Mammalian motoneuron input-output properties are strongly influenced by persistent inward currents (PICs) (Heckman & Enoka, 2012; Powers & Binder, 2001). Motoneurons integrate synaptic inputs from various sources and fire action potentials at rates proportional to the overall excitatory input (Granit, Kernell, & Lamarre, 1966). Three properties have been previously considered to be the major disruptors of the simple synaptic input-output relationship of motoneurons: Spike-frequency adaptation, spike-threshold accommodation, and PICs (Powers & Heckman, 2015; Revill & Fuglevand, 2011). Among which, PICs are accepted as a robust intrinsic property of motoneurons that are mediated by voltage-gated dendritic channels (Bennett, Hultborn, Fedirchuk, & Gorassini, 1998; Booth, Rinzel, & Kiehn, 1997; Carlin, Jiang, & Brownstone, 2000; Hounsgaard & Kiehn, 1993; Lee & Heckman, 1996) that require monoamines such as serotonin and norepinephrine to be activated (Hounsgaard, Kiehn, et al., 1988). PICs are mainly composed of L-type calcium currents (Carlin, Jones, Jiang, Jordan, & Brownstone, 2000; Hounsgaard & Kiehn, 1989) with sodium currents playing a role under specific circumstances (Y. Li et al., 2004; Manuel, Meunier, Donnet, & Zytnicki, 2007). PICs

enable the bistable behavior of motoneurons which is characterized as the continuous firing of

motoneurons even after the cessation of excitatory synaptic input (Conway, Hultborn, Kiehn, &

Mintz, 1988; Hounsgaard et al., 1984; Hounsgaard, Hultborn, et al., 1988; Lee & Heckman,

1998a). PICs can last for many seconds and have been proposed to play a role in prolonged

activity of motoneurons needed for maintenance of posture (Heckman et al., 2003; Kiehn &

Eken, 1998). Other proposed functional roles of PICs include increased excitability of

motoneurons during locomotion (Heckman et al., 2003) and normal motor behaviors

(Heckmann et al., 2005) and acting as a gain control system during a diverse range of motor

activities (Johnson & Heckman, 2014).

Although the relationship between neuromodulatory inputs and PIC characteristics have been

well studied in a variety of animal models (Bennett, Li, Harvey, et al., 2001; Bennett, Li, & Siu,

2001; Hounsgaard et al., 1984; Hounsgaard & Kiehn, 1985; Lee & Heckman, 1998b), their exact

contributions to human motor control remains unclear. Gorassini and colleagues proposed an

indirect estimate of PICs in human motoneuron discharge (M. Gorassini et al., 2002) by

measuring hysteresis, a characteristic has been associated with PICs in animal preparations

(Heckman, Johnson, Mottram, & Schuster, 2008). Because the level of excitatory inputs cannot

be directly measured in human motoneurons, they used the discharge pattern of a lower

threshold unit as a proxy to estimate the level of excitatory drive in higher threshold units. They

measured the difference in discharge frequency of a higher threshold unit in terms of a lower

threshold unit and termed it delta-frequency (ΔF). The validity of ΔF method has been

examined in rats (Bennett, Li, Harvey, et al., 2001) and in computer simulations (Elbasiouny,

Bennett, & Mushahwar, 2006; Powers & Heckman, 2015; Powers, Nardelli, & Cope, 2008; Revill & Fuglevand, 2011). Since its conception, ΔF method has been used in a number of intramuscular studies (Foley & Kalmar, 2019; Stephenson & Maluf, 2011; Vandenberk & Kalmar, 2014; Wilson et al., 2015) and surface array electrode studies (Afsharipour et al., 2020; Trajano, Taylor, Orssatto, McNulty, & Blazevich, 2020) to estimate the level of PICs in humans.

In our previous study, we investigated whether ΔF increased in proportion to voluntary effort (Kim et al., 2020). In order to maintain the duration of muscle contractions constant, ΔF values were compared at different speeds of contraction and to our surprise, the results showed that ΔF values did not change between effort levels. Previously a simulation study (Revill & Fuglevand, 2011) and an intramuscular study (Vandenberk & Kalmar, 2014) showed that faster rates of rise in current can potentially decrease ΔF estimation of PICs possibly due to spike-threshold accommodation. Spike-threshold accommodation is a progressive increase in the amount of depolarizing current required to fire an action potential during a ramp current injection, as the current injection speed decreases (Hill, 1936; Wigton & Brink, 1944). In this study, we further investigated the effects of rate of rise on ΔF and other firing properties of motor units using high-density surface array electrodes. We hypothesized that in accordance with previous studies, ΔF values would decrease as muscle contraction speeds increase. The advanced electromyography (EMG) recording technique and decomposition method based on convolutive blind source separation algorithm allowed tens of motor units to be identified per trial and provided a much deeper insight on motoneuron behaviors than previous studied. In

addition, motor units were tracked across varying contraction speeds and the effects of rate of rise on firing properties were examined.

Methods

Participants and Ethical Approval

Total of 13 (aged 23.5 ± 3.7 years, 5 females) individuals with no history of movement or neurological disorders participated in this study. After rigorous data cleaning and inclusion process, data from 11 participants (aged 23.6 ± 3.7 years, 4 females) were included in the analysis. Explanation on data inclusion criteria are further elaborated in the sections below. All procedures were performed in accordance with the Declaration of Helsinki and were approved by the Institutional Review Board at Northwestern University. All participants signed informed consent form prior to participating in the study.

Experimental Procedures

Participants were asked to sit in a Biodex experimental chair (Biodex Medical Systems, Shirley, NY) and secured with shoulder and thigh straps to minimize changes in body position. Each participant placed their left foot on an ankle attachment, which was anchored to Systems 2 Dynanometer (Biodex Medical Systems, Shirley, NY) for torque measurement. Their feet were tightly strapped to the ankle attachment by filling gaps between the feet and the straps with towels. Unless the participant expressed discomfort, the ankle was positioned at $10°$ and the knee at $20°$. Surface EMG signals were recorded from the soleus and TA muscles through 64-channel high-density surface array electrodes (HD-sEMG). The array consisted of 64 (3 rows x 5

columns) gold-coated electrodes with 1 mm diameter and 8 mm inter-electrode distance

(GR08MM1305, OT Bioelettronica, Torino, IT). Before the electrodes were applied, the skin was

shaved, slightly abraded, and cleaned with alcohol wipes. The electrodes were placed over the

medial side of soleus and the belly of TA using a bi-adhesive foam layer (KIT08MM1305, OT

Bioelettronica, Torino, IT). The skin to electrode contact was optimized by filling the wells of the

adhesive foam with conductive cream (CC1, OT Bioelettronica, Torino, IT). A strap electrode

(WS2, OT Bioelettronica, Torino, IT) was dampened and placed around the ankle of the right

foot as a ground electrode. The EMG signals were collected using OTBioLab+ software (OT

Bioelettronica, Torino, IT) in differential mode, converted to digital data by a 16-bit amplifier

(Quattrocento, 384-channel EMG amplifier, OT Bioelettronica, Torino, IT), amplified (x150),

sampled at 2048Hz, and bandpass filtered at 10-500 Hz.

After electrodes were placed, participants were asked to plantar flex and dorsiflex to their

maximum effort in an isometric condition up to three times. If one of the trials was less than

90% of the highest trial, or if the last trial was clearly the highest, another maximum voluntary

contraction (MVC) was measured. MVC was calculated by taking the mean of the three trials

with the highest MVCs. Participants were provided with a visual guidance as well as the live

feedback of their torque output. They were tasked to trace the target ramps with their torque

feedback. Depending on the trial, the peak of the ramp guidance varied between 10% and 30%

of their respective MVC and at different durations (20s, 10s, and 4s). Before data collection,

participants practiced until they were familiar with the task and able to smoothly trace the

guidance ramps to the best of their abilities. During data collection, each trial lasted about 60

seconds and participants generated two to four identical ramps depending on the duration of each ramp. For example, there were 2 ramps for 20 second ramp trials, 3 ramps for 10 second ramp trials, and 4 ramps for 4 second ramp trials. The ramps were separated by 10 second resting periods. The trials were separated by at least one-minute resting period, unless the participant asked for a longer rest. Each trial was repeated up to 3 times and the trials were presented in a randomized order.

Data Analysis

Motor Unit Decomposition and Tracking Prior to decomposition, HD-sEMG signals were visually inspected by trained study members and any channels with obvious artifacts or noise were removed. The remaining HD-sEMG data were decomposed based on convolutive blind source separation to provide motor unit spike train (Negro et al., 2016). Silhouette (SIL) values are similar to normalized measure of signal to noise ratio that are used to test the accuracy of decomposition. The SIL threshold for decomposition was set at 0.87 (Kim et al., 2020; Negro et al., 2016). After motor units were decomposed, the quality of detected motor unit spike trains was examined by expert operators and manually edited, if there were any erroneous spikes. This semi-automatic step was used to improve the accuracy of the automatic decomposition algorithm (Boccia, Martinez-Valdes, Negro, Rainoldi, & Falla, 2019; Martinez-Valdes, Negro, Falla, et al., 2020; Martinez-Valdes, Negro, Farina, & Falla, 2020).

The same motor units across different muscle contraction speeds were tracked by maximizing the cross-correlation of the motor unit action potential (MUAP) profiles (Martinez-Valdes et al.,

2017). Only motor unit matches with cross-correlation coefficient of 0.85 or greater were included in analysis.

Estimation of Persistent Inward Currents For all motor unit pair permutations, ΔF was calculated as shown in Figure 1. Subsequently, for each of the higher-threshold (test) units, we identified all paired lower-threshold (control or reporter) units which fell within the bounds of the selection criteria for ΔF calculations enumerated in detail above and in previous publications (Afsharipour et al., 2020; Kim et al., 2020; Wilson et al., 2015). The ΔF values we report are based on an average of all acceptable pairs of lower-threshold motor units with each higher-threshold motor unit. Using this "unit-wise" approach (in contrast to the "pair-wise" approach) has the benefit of being able to track individual unit ΔF values across multiple conditions and relate them to the various other motor unit firing pattern measures. Additionally, the intra-subject variability of ΔF values seems to be reduced slightly by using this method. From a theoretical perspective, the ΔF calculation necessitates similar levels of descending drive onto the two motor units used in the calculation (M. Gorassini et al., 2002; M. A. Gorassini et al., 2004). This is true for all the acceptable lower-threshold units paired with each higher-threshold motor units. Thus, it makes abundant sense from a theoretical perspective to think of ΔF as an average for each test unit.
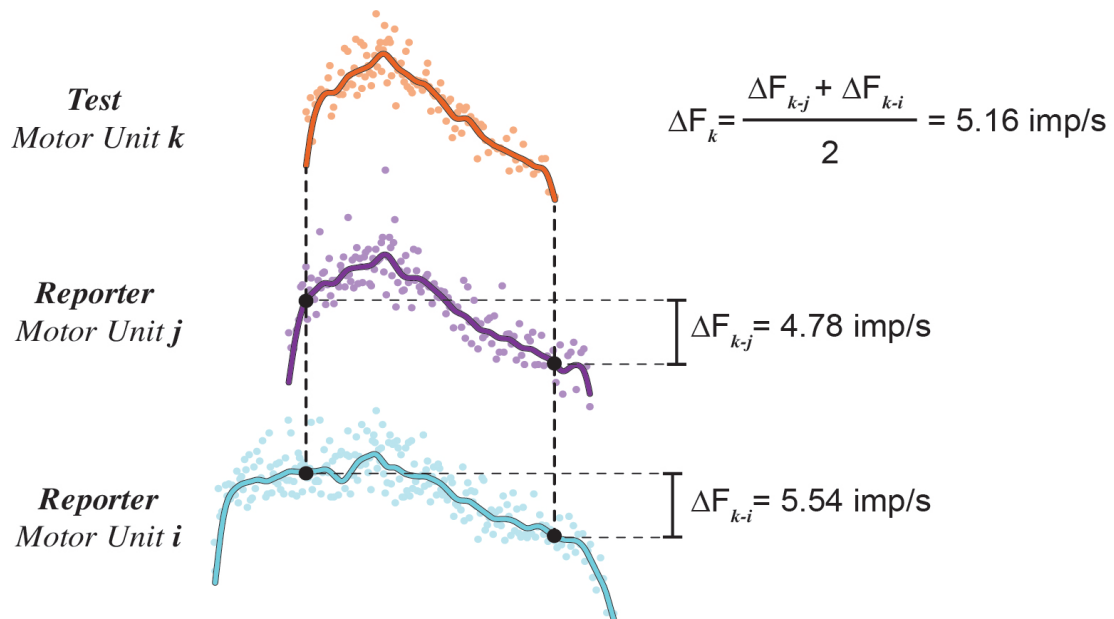
Figure 1. Unit-wise ΔF calculation example. A test unit is compared against any units with lower thresholds and ΔF's from each comparison are averaged to compute a single ΔF value. In the example, motor unit k is compared against two units with lower thresholds (motor unit j and i) and ΔF values are calculated from each comparison (4.78 and 5.54 respectively). Then, the values are averaged together and the final ΔF value for motor unit k is 5.16 imp/s.

<u>Statistical Analysis</u>

Values are reported as mean ± standard deviation (SD), unless stated otherwise. The mean values were calculated in each muscle in each subject and then averaged across subjects.

Statistical significance between mean values were computed using a linear mixed. The initial model included the interaction between %MVC, muscle contraction speed, and the interaction between them as fixed effects and subject, trial, and ramp number as random effects (on the intercept). After performing a likelihood ratio test, the results showed the interaction between %MVC and muscle contraction speed had no explanatory power. Interaction didn't matter in DeltaF (both muscles), initial firing rate (both muscles), final firing rate (TA), peak firing rate (both muscles).

DeltaF ~ %MVC + Contraction speed + (1|Subject/Trial/Ramp Number)

Post hoc analyses were conducted with the Tukey honestly significant difference test. Threshold for statistical significance was established at P < 0.05 and the effect size (ES) was estimated by Cohen's *d*.

Results

Motor Unit Yield

A total of 1285 and 1874 motor units were decomposed from the soleus and the TA muscles (128.5 ± 56.9 and 170.3 ± 101.9 per subject). From these spike trains, 3385 soleus and 3081 TA motor unit pairs had r^2 values greater than 0.7 and had at least 1 second recruitment time difference. Table 1 summarizes the total number of unit pairs included in the final analysis per muscle and per contraction speed.

Percent MVC	Muscle Contraction Speed	Soleus	TA
10% MVC	1% MVC/s	336	357
	2% MVC/s	619	483
	5% MVC/s	739	655
30% MVC	3% MVC/s	355	277
	6% MVC/s	658	601
	15% MVC/s	678	708

Table 1. Total number of motor unit pairs included in the final analysis.

Delta-F and other firing properties before matched across muscle contraction speeds

Prior to tracking motor units across various muscle contraction speeds, the mean ΔF values were calculated in each muscle in each subject and then averaged across subjects. This is the same method that we previously used to compare ΔF values from different muscles (Kim et al., 2020). Figure 2 shows that unlike our hypothesis, there is no change in ΔF across muscle

contraction speeds in the soleus. In the TA, there was a statistical increase in ΔF between 1% MVC/s and 5% MVC/s, however, no other changes are detected.
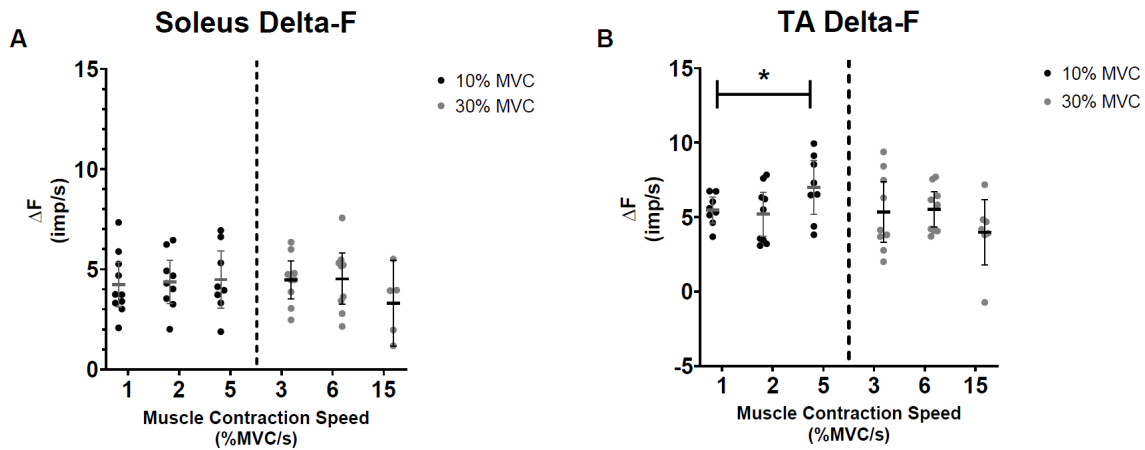

Figure 2. Delta-F before tracking. Mean (-) and standard deviation shown for ΔF values per muscle contraction speed. Each dot represents an averaged value from a single subject. (A) The mean ΔF values from the soleus at 1, 2, and 5% MVC/s (10% MVC) are 4.24 ± 1.56 imp/s. 4.38 ± 1.41 imp/s, and 4.48 ± 1.71 imp/s. The mean ΔF values from the soleus at 3, 6, and 15% MVC/s (30% MVC) are 4.47 ± 1.25 imp/s, 4.52 ± 1.67 imp/s, and 3.31 ± 1.73 imp/s. There are no statistical significance between muscle contraction speeds. (B) The mean ΔF values from the TA at 1, 2, and 5% MVC/s (10% MVC) are 5.48 ± 1.04 imp/s, 5.20 ± 1.91 imp/s, and 7.01 ± 2.18 imp/s. There is a significant increase in ΔF from 1 to 5% MVC/s. The mean ΔF values from the TA at 3, 6, and 15% MVC/s (30% MVC) are 5.33 ± 2.63 imp/s, 5.52 ± 1.56 imp/s, and 4.00 ± 2.37 imp/s and unlike 10% MVC/s, there are no statistical significance detected between muscle contraction speeds.

Figure 3 examines firing properties other than ΔF at various muscle contraction speeds. Figure 3A and 3B show as muscle contraction speed increase, there is a general increase in the initial firing rate. Figure 3C and 3D show that unlike initial firing rate, maximum firing rates do not

change across muscle contraction speeds. Figure 3E shows that with faster muscle contraction

speed, higher the final firing rate is in the soleus. Figure 3F shows that the same pattern is also

present during 10% MVC conditions, however, the statistical significance disappears during 30%
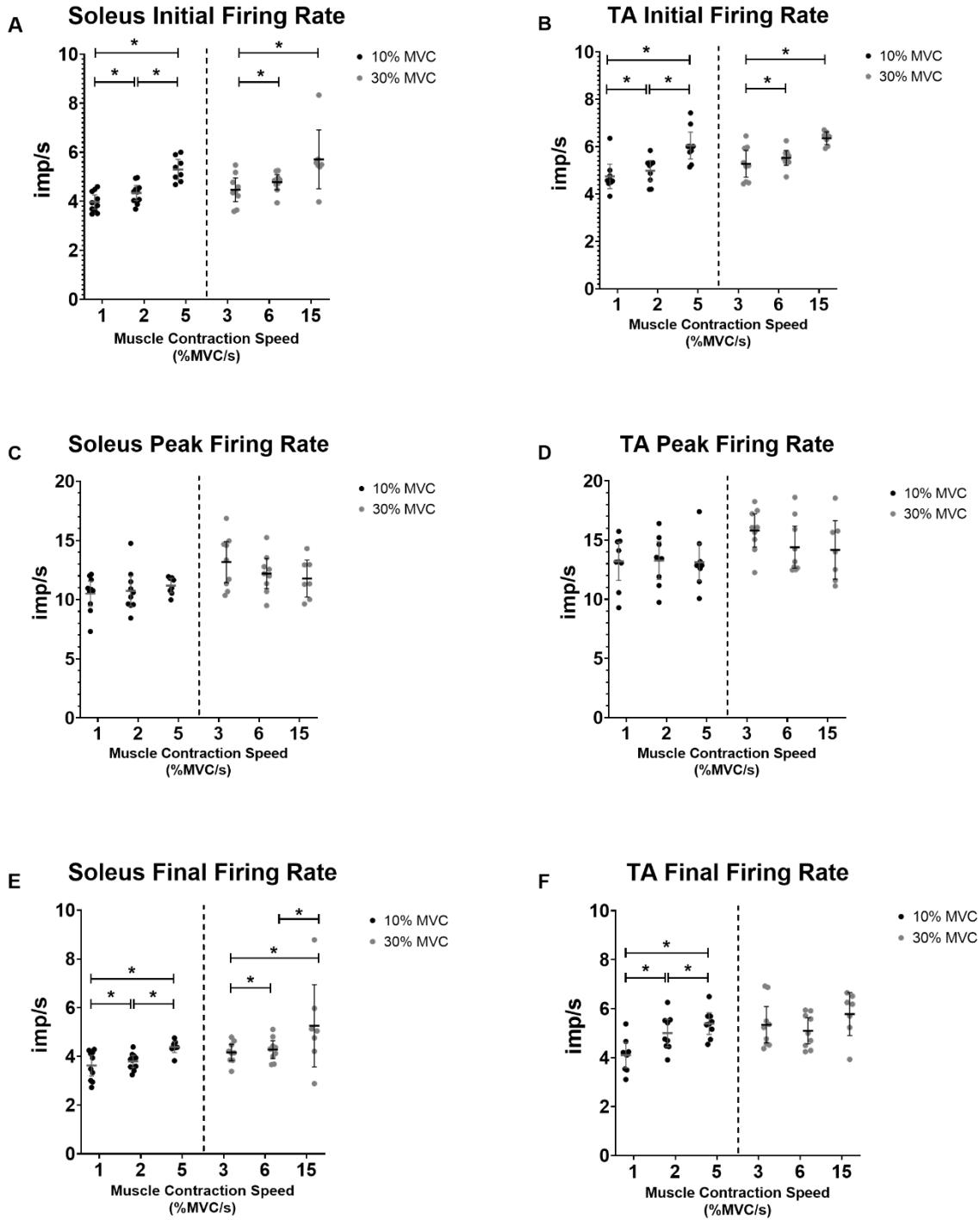
MVC conditions.

Figure 3. The effects of muscle contraction speed on different firing properties. Mean (-) and standard deviations are shown and each dot represents an averaged value from a single subject. (A) The mean initial firing rates from the soleus significantly increase from 1 to 2, 1 to 5, and from 2 to 5% MVC/s (4.00 ± 0.41 imp/s, 4.34 ± 0.43 imp/s, and 5.30 ± 0.50 imp/s). The mean initial firing rates also significantly increase from 3 to 6 and from 3 to 6%MVC/s, however not from 6 to 15% MVC/s (4.47 ± 0.62 imp/s, 4.78 ± 0.40 imp/s, and 5.71 ± 1.30

imp/s). (B) The mean initial firing rates from the TA also significantly increase from 1 to 2, 1 to 5, and from 2 to 5% MVC/s (4.78 ± 0.67 imp/s, 4.99 ± 0.56 imp/s, and 6.05 ± 0.74 imp/s). Just like the soleus, the mean initial firing rates also significantly increase from 3 to 6 and from 3 to 6%MVC/s, however not from 6 to 15% MVC/s (5.28 ± 0.73 imp/s, 5.53 ± 0.41 imp/s, and 6.35 ± 0.29 imp/s). (C) The mean peak firing rates from the soleus does not change significantly as muscle contraction speed increases. From left to right, the mean peak firing rates at 1, 2, 5, 3, 6, 15% MVC/s are 10.51 ± 1.48 imp/s, 10.73 ± 1.77 imp/s, 11.18 ± 0.73 imp/s, 13.17 ± 2.25 imp/s, 12.20 ± 1.65 imp/s, and 11.78 ± 1.70 imp/s. (D) The mean peak firing rates from the TA also does not change significantly as muscle contraction speed increases. From left to right, the mean peak firing rates at 1, 2, 5, 3, 6, 15% MVC/s are 13.21 ± 2.10 imp/s, 13.27 ± 2.07 imp/s, 13.13 ± 2.04 imp/s, 15.81 ± 1.83 imp/s, 14.40 ± 2.31 imp/s, 14.17 ± 2.67 imp/s. (E) As muscle contraction speed is increased, the final firing rates from the soleus are also increased significantly. From left to right of the graph, the mean final firing rates are 3.62 ± 0.60 imp/s, 3.80 ± 0.34 imp/s, 4.40 ± 0.27 imp/s, 4.16 ± 0.44 imp/s, 4.28 ± 0.48 imp/s, and 5.25 ± 1.83 imp/s. (F) As muscle contraction speed is creased, the final firing rates from the TA are significantly increased during 10% MVC condition, but not 30% MVC. The mean final firing rates during 10% MVC are 4.10 ± 0.67 imp/s, 5.00 ± 0.73 imp/s, and 5.40 ± 0.57 imp/s at 1, 2, and 5 %MVC/s. The mean final firing rates during 30% MVC are 5.34 ± 0.96 imp/s, 5.10 ± 0.70 imp/s, and 5.78 ± 0.95 imp/s at 3, 6, and 15 % MVC/s.

ΔF vs Recruitment Torque

Figure 4 illustrates how ΔF varies across different recruitment torques and simple linear regression lines are fitted to measure if the slope is significantly non-zero. Figure 4A and 4B show that except for the 6% MVC/s condition, there is generally no change in ΔF across motor units from different recruitment torques in the soleus. Figure 4C and 4D show that the results are a little more mixed in the TA. During 2%, 3% and 6% MVC/s conditions, ΔF's significantly decrease as the recruitment torque increase.
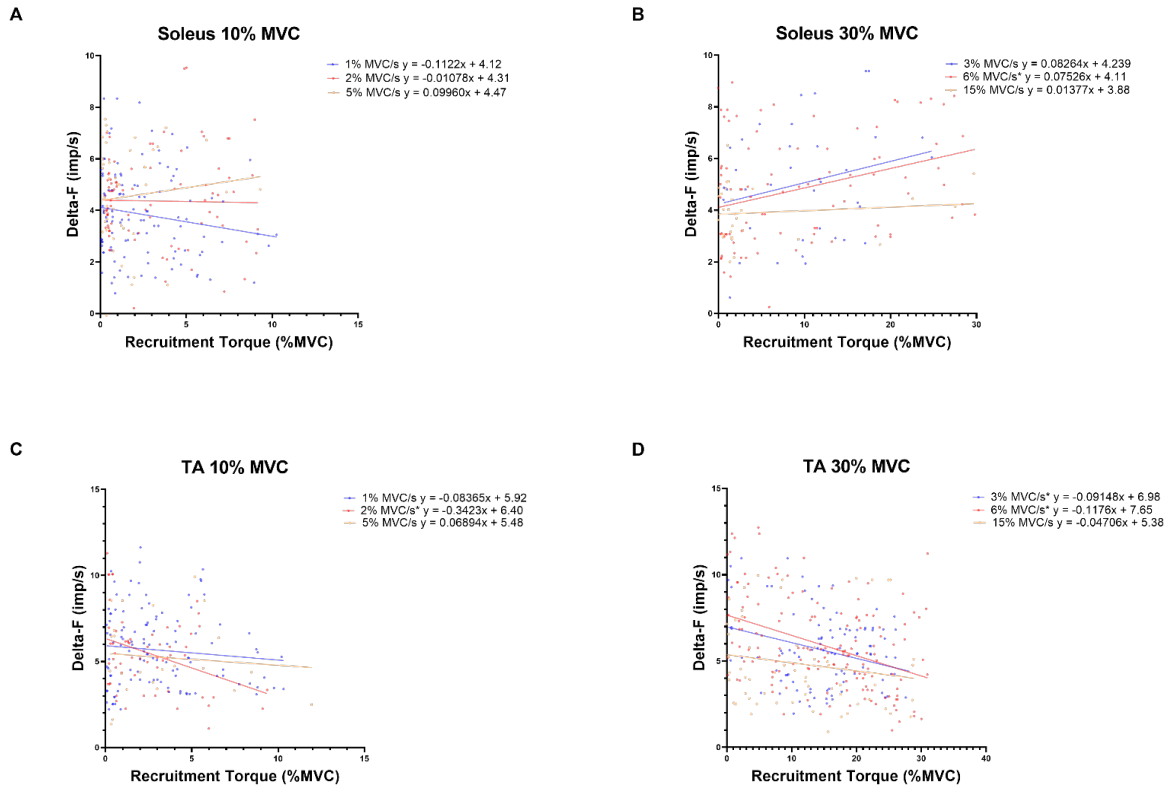
A Soleus 10% MVC

1% MVC/s y = -0.1122x + 4.12
2% MVC/s y = -0.01078x + 4.31
5% MVC/s y = 0.09960x + 4.47

B Soleus 30% MVC

3% MVC/s y = 0.08264x + 4.239
6% MVC/s* y = 0.07526x + 4.11
15% MVC/s y = 0.01377x + 3.88

C TA 10% MVC

1% MVC/s y = -0.08365x + 5.92
2% MVC/s* y = -0.3423x + 6.40
5% MVC/s y = 0.06894x + 5.48

D TA 30% MVC

3% MVC/s* y = -0.09148x + 6.98
6% MVC/s* y = -0.1176x + 7.65
15% MVC/s y = -0.04706x + 5.38

Figure 4. Delta-F vs Recruitment Torque. Each dot represents a ΔF value of a single motor unit calculated using unit-wise method. (A) Under 10% MVC condition, there is no change in ΔF values in the soleus among units recruited at different torques. (B) Under 30% MVC condition, ΔF increases with increasing recruitment torque if the soleus is contracted at 6% MVC/s ($p = 0.0055$). However, ΔF does not change if it is contracted at 3 or 15% MVC/s. (C) Under 10% MVC condition, ΔF decreases with increasing recruitment torque if the TA is contracted at 2% MVC/s ($p = 0.0066$). However, ΔF does not change at 1 and 5% MVC/s contraction speeds. (D) With higher recruitment torques, ΔF decreases if the TA is contracted at 3 and 6% MVC/s ($p = 0.0058$ and $p < 0.0001$). On the other hand, ΔF does not change at 15% MVC/s contraction speed.

Motor Unit Tracking

Figure 5 shows an example of a single unit tracked across three different muscle contraction speeds by maximizing the cross-correlation of the motor unit action potential (MUAP) profiles. A total of 403 individual units (185 soleus and 218 TA) were tracked across at least two contraction speeds. The minimum requirement for the cross-correlation coefficients between

matched units was 0.85 and the average cross-correlation coefficient for matched units included in final analysis was 0.91.

ΔF and other firing properties after matched across muscle contraction speeds

In accordance with the unmatched data, ΔF values did not change significantly with varying muscle contraction speeds even after matched (Figure 6). The results from other firing properties were also similar to those from unmatched data. Figure 7A and 7B show that as muscle contraction speed increases, same units start firing at a higher frequency in both soleus and the TA muscles. Figure 7C and 7D show that although motor units increase initial firing rates with contraction speed, there are no changes in peak firing rates. Figure 7E and 7F show that similar to unmatched data, there is a general trend of increase in final firing rate as the muscle contraction speed increases.

Figure 5. Example of motor unit tracking. Motor units were tracked across different muscle contraction speeds by maximizing the cross-correlation of the motor unit action potential profiles. In the representative figure, the cross-correlation coefficients between 1 and 2, 2 and 5, and 1 and 5% MVC/s are 0.94, 0.90, and 0.91.
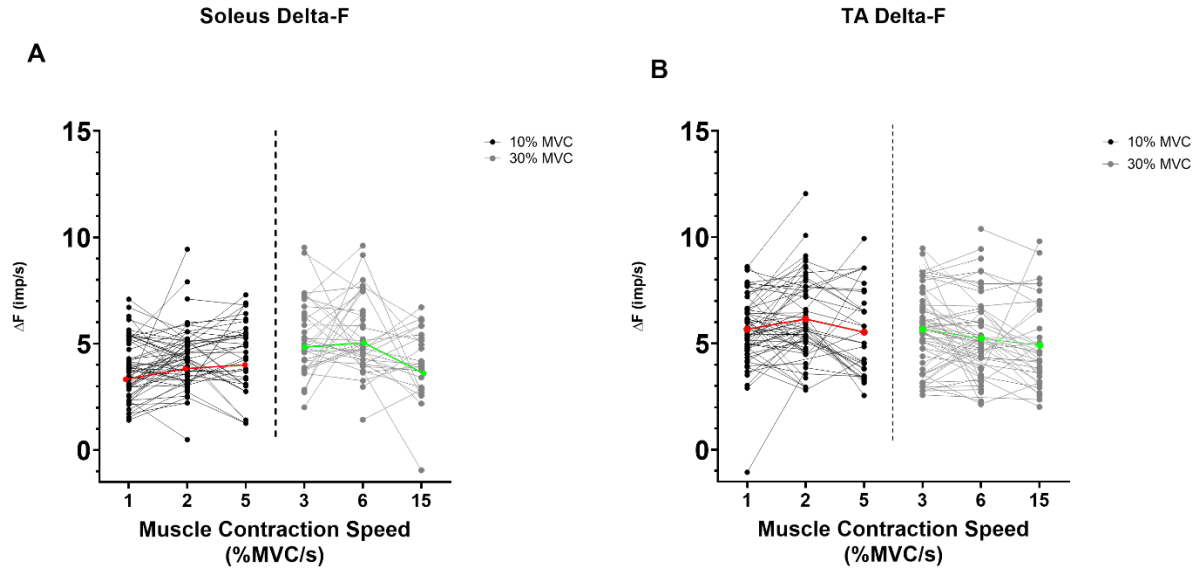
Figure 6. Delta-F after matching. Same motor units are connected with a line and ΔF values are tracked across varying muscle contraction speed. The results show no changes are statistically meaningful from both muscles. (A) The mean ΔF values from the soleus at 1, 2, and 5% MVC/s (10% MVC) are 3.81 ± 1.39 imp/s, 4.30 ± 1.42 imp/s, and 4.48 ± 1.66 imp/s. The mean ΔF values from the soleus at 3, 6, and 15% MVC/s (30% MVC) are 5.30 ± 1.77 imp/s, 5.50 ± 1.82 imp/s, and 4.08 ± 1.66 imp/s. (B) The mean ΔF values from the TA at 1, 2, and 5% MVC/s (10% MVC) are 5.66 ± 1.66 imp/s, 6.14 ± 1.94 imp/s, and 5.51 ± 2.02 imp/s. The mean ΔF values from the TA at 3, 6, and 15% MVC/s (30% MVC) are 5.65 ± 1.83 imp/s, 5.22 ± 1.83 imp/s, and 4.90 ± 1.97 imp/s.
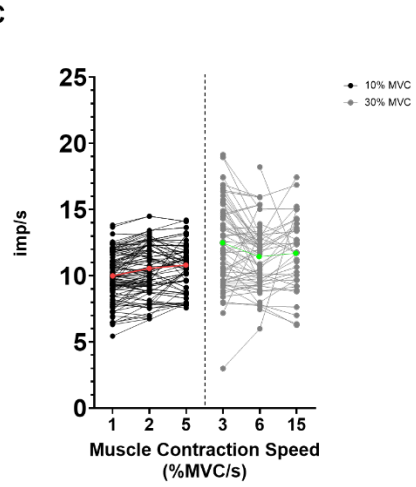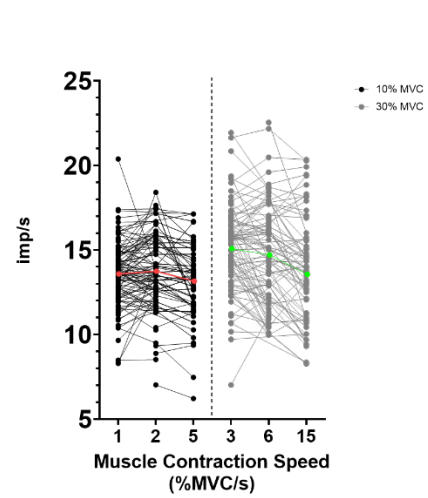
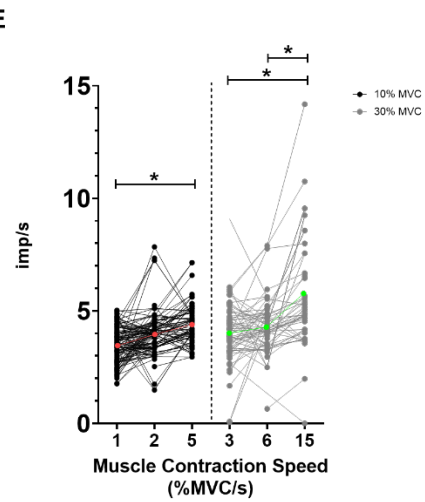**Soleus Initial Firing Rate**

A
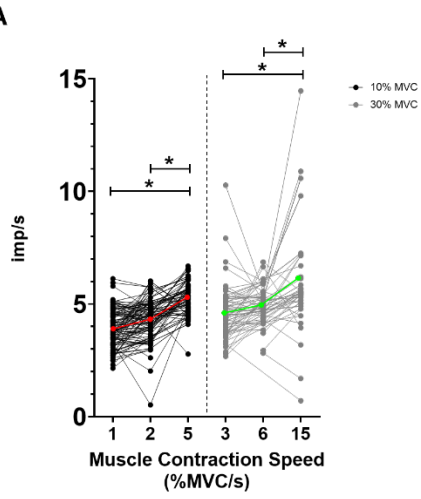
TA Initial Firing Rate

B
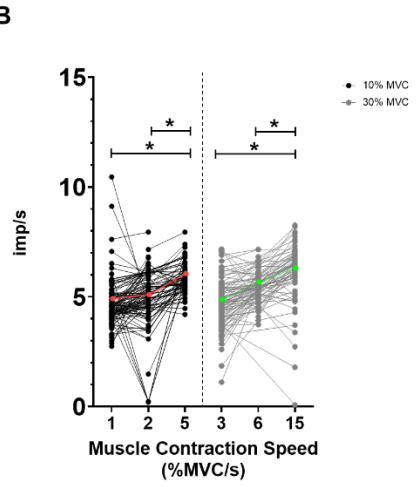
Soleus Peak Firing Rate

C

TA Peak Firing Rate

D

Soleus Final Firing Rate
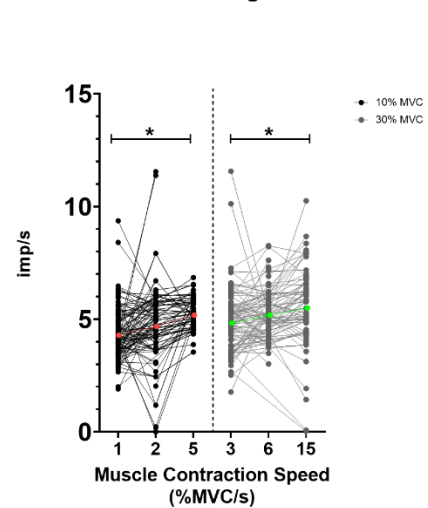
E

TA Final Firing Rate

F

Figure 7. The effects of muscle contraction speed on firing properties per motor unit. Same motor units are connected with a line and ΔF values are tracked across varying muscle contraction speed. (A) The mean initial firing rates from the soleus significantly increase as muscle contraction speed increases. From left to right of the graph, the mean initial firing rates are 3.88 ± 0.84 imp/s, 4.32 ± 0.88 imp/s, 5.31 ± 0.70 imp/s, 4.61 ± 1.24 imp/s, 4.97 ± 0.76 imp/s, and 6.18 ± .36 imp/s. (B) The mean initial firing rates from the TA also significantly increases as muscle contraction speed increases. The mean initial firing rates are 4.71 ± 1.08 imp/s, 4.90 ± 1.35 imp/s, 5.87 ± 0.66 imp/s, 4.68 ± 1.10 imp/s, 5.49 ± 0.73 imp/s, and 6.13 ± 1.27 imp/s. (C) Similar to the results from unmatched data, muscle contraction speed has no effect on peak firing rates of the soleus muscle. The peak firing rates are 9.95 ± 1.78 imp/s, 10.52 ± 1.85 imp/s, 10.77 ± 1.68 imp/s, 12.48 ± 3.29 imp/s, 11.41 ± 2.42 imp/s, and 11.68 ± 2.80 imp/s. (D) Muscle contraction speed also does not have any effect on the peak firing rates of the TA muscle. At 1, 2, 5 (10% MVC) and 3, 6, 15 (30% MVC) % MVC/s, their firing rates were 13.60 ± 1.93 imp/s, 13.77 ± 2.13 imp/s, 13.17 ± 2.07 imp/s, 15.10 ± 2.50 imp/s, 14.73 ± 2.94 imp/s, 13.58 ± 3.03 imp/s. (E) It is shown that just like in unmatched data, increasing muscle contraction speed also increases final firing rates in the soleus muscle. A statistical significance is reached between 1 and 5 %MVC/s for 10% MVC and 3 and 15, and 6 and 15 %MVC/s for 30% MVC. Their firing rates are 3.46 ± 0.79 imp/s, 3.97 ± 0.96 imp/s, 4.41 ± 0.82 imp/s, 4.03 ± 1.36 imp/s, 4.30 ± 1.17 imp/s, and 5.81 ± 2.48 imp/s. (F) It is also shown that increasing muscle contraction speed increases final firing rates in the TA muscle. A statistical significance is reached between 1 and 5% MVC/s and 3 and 15% MVC/s. Their firing rats are 4.37 ± 1.17 imp/s, 4.77 ± 1.70 imp/s, 5.27 ± 0.72 imp/s, 4.91 ± 1.42 imp/s, 5.27 ± 1.07 imp/s, and 5.59 ± 1.66 imp/s.

Discussion

Advantages of tracking method

Our data showed that the results from grouped data (untracked) and tracked data were very similar. There were no changes in ΔF across muscle contraction speeds, an increase in initial firing rate, no change in peak firing rate, and an increase in final firing rate. However, grouped data only show trends and cannot answer whether the changes in motor unit firing patterns are due to recruitment of new units or changes in firing behavior of already recruited units. Recruitment and rate coding are the two main strategies for motor units to control force output and the relative contribution of these strategies depends on the muscle and its functions. A previous intramuscular study has reported that during a medium-speed ramp contraction

(approximately 10%MVC/s), high threshold units in the soleus muscle are not recruited until close to MVC. Therefore, the authors concluded that the soleus muscle utilizes both recruitment and rate coding over the full range of force output rather than solely relying on rate coding at high forces (Oya, Riek, & Cresswell, 2009). In this study, we tracked a large number of soleus and TA motor units across varying contraction speeds and the results clearly showed the changes in firing properties of units recruited up to 30% MVC can be attributed to rate coding, rather than recruitment. Oya and Cresswell showed the recruitment threshold of soleus motor units is widely distributed across MVC's (Figure 2 of Oya and Cresswell 2009). The same figure also showed that the number of recruited units decrease from 0%MVC to 40% MVC. It is possible that for motor tasks that require less than 40% MVC the soleus relies more on rate coding while reserving higher threshold units for motor tasks that require higher force output.

No changes in ΔF across muscle contraction speeds

One of the central questions this study aimed to answer was whether muscle contraction speeds have any effects on ΔF. Previous simulation and intramuscular studies have shown that faster rate of rise can decrease ΔF estimation of PICs through spike-threshold accommodation (Revill & Fuglevand, 2011; Vandenberk & Kalmar, 2014). Therefore, we hypothesized that our array data would also show that ΔF would decrease as muscle contraction speed increased. However, the results showed that unlike our hypothesis, there were no changes in ΔF across varying muscle contraction speeds. The disparity between the results from previous studies and this study could be due to difference in data collection methods. Vandenberk and Kalmar

measured the changes in ΔF after varying muscle contraction speeds from approximately

1%MVC /s to 2%MVC/s in the TA muscle (Vandenberk & Kalmar, 2014). They used

intramuscular electrodes to collect and record 14 – 15 motor units from 14 subjects and after

pairwise ΔF analysis, reported a decrease in ΔF with an increase in rate of rise. Although

intramuscular recording and pairwise ΔF analysis were widely used in the past to estimate PICs

in humans, recent studies have shown that they result in a high variability (Afsharipour et al.,

2020; Hassan et al., 2020). High-density surface array EMG recordings deliver a much larger

number of motor units which allows significantly higher number of permutations for ΔF

calculation and more reliable results. Also, in this study, unit-wise comparison was used to

estimate PICs instead of pairwise comparison. Unit-wise comparison uses multiple ΔF values to

represent an average ΔF each unit and it reflects a more representative descending drive to the

motor unit than pair-wise comparison.

Revill and Fuglevand observed an increase in initial firing rate with their simulation model due

to spike threshold accommodation. However, they observed no change in final firing rate (Revill

& Fuglevand, 2011). On the other hand, another simulation study with more physiologically

agreeable model showed when spike threshold accommodation was present, motor units were

de-recruited earlier with higher ramp speed (Powers & Heckman, 2015). Our tracked and

untracked data showed results similar to the latter study: With an increase in muscle

contraction speed, there was an increase in initial firing rate and in final firing rate, rendering

no change in overall ΔF. Later sections will further discuss what could have caused the changes

in motor unit firing behaviors.

No change in ΔF across different recruitment thresholds

Figure 4 illustrated that there was no change in ΔF across recruitment torque and similar results were also reported in a recently published study (Figure 9 of Afshariopour et al 2020). According to Henneman's size principle, motor units are recruited based on order of their sizes with smaller units recruited first and larger units recruited later. Our data and the recent publication suggested there was no difference in the level of PICs for motor units recruited up to 30% MVC in the TA and the soleus muscles. However, Afshariopour et al. speculated there might be a subthreshold activation of PICs especially in smaller units and ΔF underestimates true level of PICs. They observed larger units start firing at a much lower frequency and increase firing rate relatively slowly over 2-3 seconds. This slow increase in firing rate reflected slow activation of PICs as Ca-PICs take few seconds to be fully activated due to L-type calcium channel dimerization (Binder, Powers, & Heckman, 2020). This suggested there was no substantial amount of subthreshold activation of PICs in larger units and ΔF values were truthful. On the other hand, they observed a higher initial firing rate and a relatively short activation period (referred to as "secondary range" by Wienecke et al 2008 and Afshariopour et al 2020 and as "acceleration" by Johnson et al 2017) for smaller units which suggest subthreshold activation PICs (Afsharipour et al., 2020; Johnson, Thompson, Tysseling, Powers, & Heckman, 2017; Wienecke, Zhang, & Hultborn, 2009). Our results further reinforced the possibility of subthreshold activation of PICs in smaller units and more investigation is needed to accurately quantify secondary range in motor units.

Increase in initial firing rate

Tracked and untracked data showed a significant increase in initial firing rate as muscle contraction speed increased. Similar results were also reported in a study that measured firing frequency of TA motor units during ballistic contractions (Desmedt & Godaux, 1976). As mentioned above, higher initial firing rate can be partly explained by subthreshold activation of PICs and the first spike represents already boosted motor output. Subthreshold activation of plateau potential has been reported in decerebrate cats and in vitro and intact rat preparations (Bennett et al., 1998; Bennett, Li, & Siu, 2001; M. Gorassini, Bennett, Kiehn, Eken, & Hultborn, 1999; M. Gorassini, Eken, Bennett, Kiehn, & Hultborn, 2000). Another possible explanation for an increase in initial firing rate is a stronger synaptic excitation due to descending inputs from the cortex. Especially during high muscle contraction speeds, it is unlikely that Ca-PICs are fully activated. PICs are thought to be involved in postural control which is usually a slow and steady movement (Brownstone, 2006; Heckman, Mottram, Quinlan, Theiss, & Schuster, 2009; Johnson & Heckman, 2010). It is possible that the descending inputs from the cortex are more heavily involved than the ones from the brainstem during motor tasks that require faster muscle contractions.

No change in peak firing rate

According to the Onion-Skin scheme, later recruited units have lower peak firing rate than earlier recruited units (De Luca & Erim, 1994). If the increase in initial firing rate accompanied by increase in muscle contraction speed was achieved by recruiting higher threshold units, it would decrease peak firing rate. However, that was not the case and although there was a

minor trend of decrease in peak firing in the TA (Figure 3D and Figure 7D), it was not strong

enough to reach a statistical significance. Peak firing rate indicates the overall strength of

descending inputs (corticospinal and bulbospinal combined) to motor pool. Taken together with

no changes in ΔF, increasing muscle contraction speeds does not require more overall

descending inputs to the motoneuron pool. However, it doesn't exclude the possibility that

individual contribution of corticospinal and bulbospinal descending inputs might vary

depending on contraction speed. It is also noteworthy that the peak firing rates might have

been underestimated during high contraction speeds. The duration for the ascending limb of

high-speed ramps was 2 seconds which would be difficult for PICs to be fully activated for units

that were recruited later.

Increase in final firing rate

Final firing rate was significantly increased in both the soleus and TA muscles as contraction

speed increased (Figures 3E, 3F, 7E, and 7F). In cat preparations, Wienecke and colleagues

observed lower firing rates at derecruitment than recruitment during triangular current

injections (Wienecke et al., 2009). The authors showed a prolongation of the

afterhyperpolarization (AHP) duration after a ramp-current injection. The AHP is caused by a

potassium current that is evoked by calcium influx during the action potential (Hounsgaard,

Kiehn, et al., 1988; Krnjević, Puil, & Werman, 1978; P. C. Schwindt, Spain, & Crill, 1984). They

speculated calcium buildup after a long train of action potentials in combination with Ca-PICs as

the reason for a prolongation of the AHP duration. In our experiment, ramp durations were

much shorter during fast contractions compare to slow contractions. This could have led to a

less-buildup in calcium at the site of the channels and a shorter prolongation of the AHP

duration, which in turn caused an increase in final firing rate.

Conclusion

In conclusion, with increasing muscle contraction speed, we observed no changes in ΔF and

peak firing rates but an increase in initial and final firing rates. The results implied that

increasing muscle contraction speed was not accompanied by increasing monoaminergic input

from the brainstem. However, increase in initial firing rate could have been due to an increase

in inputs from the cortex. One limitation of the ΔF method that the study revealed was due to

high variability in ΔF, motor unit pairs with less than 1 second recruitment time difference

could not be included in analysis (Hassan et al., 2020). This was especially problematic when

calculating ΔF during rapid contractions that last less than 2 seconds because it only allowed a

small fraction of the recruited motor units to be included in the analysis. We overcame this

challenge by using HD-sEMG to decompose a large number of motor units. Another limitation

during the high-speed contractions was the difficulty analyzing firing patterns of high-threshold

units due to their short active periods. In the future, more studies should focus on improving ΔF

methods for high-contraction speeds and analyzing firing patterns of high-threshold units.

CHAPTER III. Properties of Motor Units of Ankle Muscles Decomposed Using High-Density

Surface EMG

Abstract

Analyses of motor unit activity provide a window to the neural control of motor output. In

recent years, considerable advancements in surface EMG decomposition methods have allowed

for the discrimination of dozens of individual motor units across a range of muscle forces. While

these non-invasive methods show great potential as an emerging technology, they have

difficulty discriminating a representative sample of the motor pool. In the present study, we

investigate the distribution of recruitment thresholds and motor unit action potential

waveforms obtained from high density EMG across soleus and tibialis anterior. Five young and

healthy control subjects generated isometric torque ramps between 10-50% maximum

voluntary torque during ankle flexion and extension. Hundreds of motor units were

decomposed for each muscle across all trials. For lower contraction levels and speeds, surface

EMG decomposition discriminated a large number of low-threshold units. However, during

contractions of greater speed and torque level the proportion of low threshold motor units

decomposed was reduced, resulting in a relatively uniform distribution of recruitment

thresholds. The number of motor units decomposed decreased as the contraction level and

speed increased. The decomposed units showed a wide range of recruitment thresholds and

MUAP amplitudes. In conclusion, although surface EMG decomposition is a useful tool to study

large populations of motor units, data from such attempts should be interpreted in the context

of limitations in sampling of the motor pool.

Introduction

Investigation of motor unit activity in humans affords a more comprehensive view of the neural drive underlying motor output. Traditionally, motor unit recordings were carried out with intramuscular concentric needle or fine wire electrodes. Though these invasive approaches are used in both clinical and research settings, they are usually only effective during low levels of muscle contraction due to the increased superimposition of motor unit action potentials (MUAPs) at higher forces. Further, these methods show high selectivity, can usually only detect a handful of motor units, and often require a trained operator to discriminate individual MUAPs. All of these factors have been a major hurdle in clarifying fundamental questions about the neural control of motor output (Duchateau & Enoka, 2011). In recent years, decomposition algorithms utilizing high-density surface EMG arrays have allowed for non-invasive recordings from a larger population of motor units, across a wider range of contraction levels, and with greater efficiency (Holobar, Minetto, & Farina, 2014; Negro et al., 2016). These advancements have made it possible to detect dozens of motor units during the same contraction.

Despite these obvious advantages, investigators using these methods must remain aware that surface EMG decomposition may not provide a representative sample of motor units from all muscles. When recording from the skin, the ability to decompose a motor unit is based on the statistical characteristics (spatial and temporal) (Martinez-Valdes et al., 2017) and the surface energy of its action potentials (Holobar, Farina, Gazzoni, Merletti, & Zazula, 2009). This may impede identification of lower-amplitude smaller MUAPs, including those originating deeper within the muscle. Additionally, the number of active motor units comprising the EMG signals

may reduce the capacity of the decomposition approaches to separate the contribution of individual units, though to a lesser degree than conventional intramuscular single motor unit analysis techniques.

The goal of the present study was to investigate the distribution of motor unit recruitment threshold and MUAP amplitude in a large sample of recordings from the soleus (SOL) and the tibialis anterior (TA), using an automatic high-density surface EMG decomposition approach previously published (Martinez-Valdes et al., 2017; Negro et al., 2016). According to Henneman's size principle, smaller motor units are recruited before their larger counterparts due to the intrinsic electrophysiological properties of motor (HENNEMAN et al., 1965). Fine wire analysis has shown that the number of motor units recruited decreases exponentially as force increases, including muscles reported in this paper (Feiereisen, Duchateau, & Hainaut, 1997; Kukulka & Clamann, 1981; Milner-Brown et al., 1972; van Groeningen & Erkelens, 1994). Similarly, Oya and colleagues discovered that in the SOL, the number of recruited units decreases as the torque level increases until about 50% MVT and increases afterward (Oya et al., 2009). This is consistent with the notion of a relatively large number of slow motor units with fewer large motor units (Enoka & Fuglevand, 2001). Our current results are contrary to this expectation. However, a moderate level of correlation between MUAP amplitude and force recruitment threshold has been shown previously (Del Vecchio, Negro, Felici, & Farina, 2017; Martinez-Valdes, Negro, Falla, De Nunzio, & Farina, 2018) and, as stated above, the decomposition algorithm may be biased by MUAP amplitude. For the higher contraction levels, the distribution of motor unit recruitment threshold was relatively uniform. The number of

motor units identified was muscle dependent and decreased considerably at higher torque levels. These factors should be considered in the interpretation of results discriminated from surface EMG decomposition methods.

Methods

Participants

Five healthy adults (aged 25.6 ± 3.3, 40% female, 730 units from the soleus, 960 units from the TA) participated in the experiments. All participants reported having no known neurological or motor impairments. All participants provided informed consent prior to participation in these experiments, which were approved by the Institutional Review Board of Northwestern University (IRB Number: STU00202964).

Experimental Apparatus

Participants were seated in a Biodex experimental chair (Biodex Medical Systems, Shirley, NY) and secured with shoulder and thigh straps. Each participant's dominant foot was strapped to an ankle attachment, which was attached to Systems 2 Dynanometer (Biodex Medical Systems, Shirley, NY) to measure the ankle torque. Unless participant expressed discomfort, the ankle was positioned at an angle of 100° and the knee were positioned at an angle of 160°.

Bipolar surface EMG recordings were collected from the soleus (Sol) and the tibialis anterior

(TA) using grids of 64 electrodes, with 8mm inter-electrode distance. The signals were amplified

(x150), band-pass filtered (10-500Hz) and sampled at 2048 Hz (EMG-USB2 for 2 lower limb

subjects and Quattrocento for rest, OT Bioelettronica, Turin, IT).

Protocol

Participants were asked to generate maximum voluntary torques (MVTs) during ankle dorsiflexion and plantarflexion. Trials within a direction were repeated until three trials with peaks within 10% of the maximum torque were collected. Participants were provided with enthusiastic vocal encouragement, as well as real time visual feedback during MVT trials.

Figure 1. Isometric joint torque recording device with high-density surface EMG grids on the soleus and tibialis anterior muscles.

Experimental trials entailed the generation of triangular isometric torque ramps. Participants

were instructed to gradually increase their dorsiflex/plantarflex about the ankle to 10%, 30%, or

50% MVT over 10 seconds, followed by gradually relaxing back to baseline over 10 seconds.

Trials consisted of either two or three ramps with ten seconds between ramps and five seconds

of baseline at the beginning and end of each trial.

Participants were given a few practice trials to become comfortable with the task followed by

five to six experimental trials. Torque traces were visually inspected and trials with large

deviations from the desired time-torque profile were discarded.

Data Analysis

All surface EMG channels were visually inspected and those with substantial artifacts or noise were removed. The remaining surface EMG channels were analyzed based on convolutive blind source separation to provide motor unit spike trains (Negro et al., 2016). The silhouette threshold for decomposition was 0.87. All motor units were manually inspected by experienced investigators and only reliable discharge patterns with physiological variability were considered for the analysis.

In order to eliminate any possible duplicate motor units, motor units within the same muscle and trial were cross correlated. If any motor u

nit pairs shared more than a 30% overlap in spike times, the motor unit with the higher covariance value was removed. MUAPs were reconstructed based on spike-triggered averaging of each of the surface EMG channels in the high-density surface array grid. The root mean square (RMS) amplitude of the MUAP was calculated over a 25 ms window within each channel. In order to reduce inter-subject variance, the RMS amplitudes of the reconstructed MUAPs were all normalized to the maximum RMS MUAP amplitude seen during the highest contraction level trials, within each subject.

Statistical Analysis

Values are presented as means $\pm$ standard deviation (SD). For all distributions shown, normality was assessed using the Kolmogorov-Smirnov assess normality. Kurtosis and skewness were used to quantify the tailedness and asymmetry, respectively, of the distributions. Wilcoxon

rank-sum was performed to compare MUAP RMS values between contraction levels within the SOL and the TA, as it is not dependent on normality. A confidence level of $p < 0.05$ was considered statistically significant.

Results

Number of decomposed motor units

Figure 2 shows firing patterns of motor units during a typical trial. Shown here are 14 units from the TRI with wide range of recruitment thresholds that were collected and decomposed. The black line represents the torque generated by the subject under 20% MVT condition. A total of 730 and 960 motor unit spike trains were decomposed and analyzed for the SOL and TA, respectively. For 10% MVT, 286 and 338 motor unit spike trains were analyzed; for 30% MVT, 253 and 355 motor unit spike trains were analyzed; and for 50% MVT, 191 and 267 motor unit spike trains were analyzed, for the SOL and TA respectively. A total of 445 motor unit spike trains were analyzed for the BIC and 930 for the TRI.
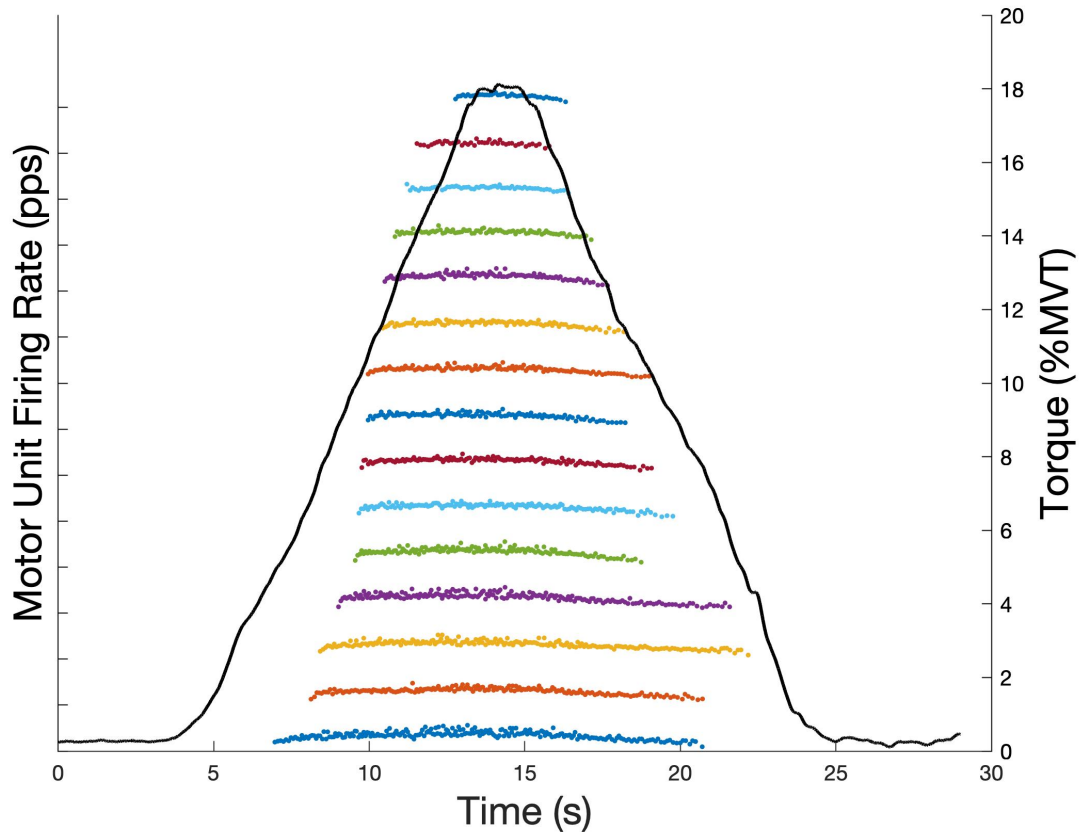
Figure 2. The firing patterns of 14 motor units decomposed from during a single trial, along with the torque trace (black). For scale, the ticks on the left y-axis are spaced at 50 pps apart.

Recruitment threshold

Figure 3 shows the distributions of %MVT at motor unit recruitment from all four muscles during different %MVT ramps. The average recruitment threshold for 10% MVT per subject is 4.4 ± 3 %MVT for the SOL and 2.7 ± 3.3 %MVT for the TA. The average recruitment threshold for 30% MVT per subject is 16.9 ± 8.3 %MVT for the SOL and 10.2 ± 10.6 %MVT for the TA. Finally, the average recruitment threshold for 50% MVT per subject is 28.5 ± 12.8 %MVT for the SOL and 17.9 ± 17.6 %MVT for the TA. The skewness and kurtosis for these distributions is showed in Table 2. Additionally, according to Kolgomorov-Smirnov test none of this data followed a normal distribution.

Muscle	%MVT	Skewness	Kurtosis
Soleus	10	0.41	2.1
	30	-0.21	1.9
	50	-0.26	2.1
TA	10	1.1	3.4
	30	0.44	1.7
	50	0.31	1.6

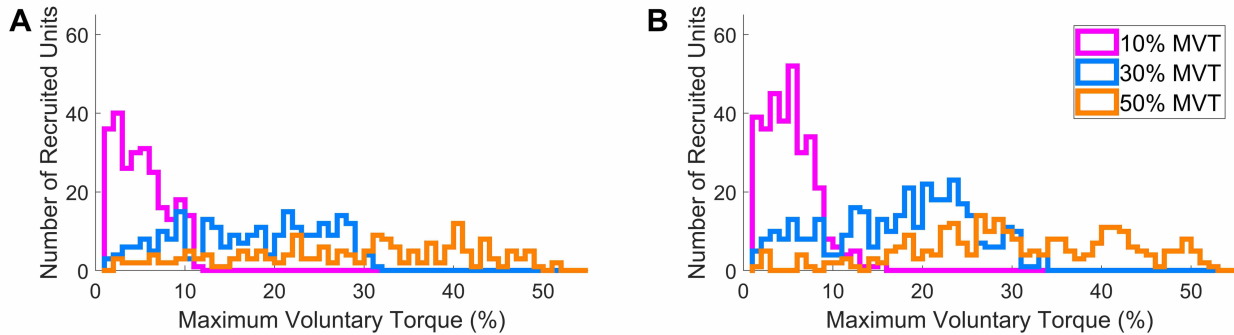**Table 1**. Recruitment Threshold Distributions

Figure 3. Motor unit recruitment threshold during 10%, 30%, and 50% MVT for soleus and TA.

MUAP Amplitude

Figure 4 shows normalized the root-mean-squared amplitudes of MUAPs from all four muscles. There is no unit because all the values are normalized. The average MUAP RMS amplitude at 10% MVT for the SOL and TA are 0.35 ± 0.25 and 0.21 ± 0.16, respectively. The same measurement for 30% MVT is 0.36 ± 0.21 in the SOL and 0.29 ± 0.19 in the TA. For 50% MVT, the average distributions of MUAP RMS amplitude are 0.43 ± 0.20 in the TA and 0.41 ± 0.24 in the SOL. For the TA and SOL, the distribution of MUAP amplitudes is skewed to the right, across all contraction levels and speeds. The median MUAP amplitudes for the SOL are 0.28, 0.33, and 0.39 at 10%, 30%, and 50%. The median MUAP amplitudes for the TA are 0.17, 0.27, and 0.43 at 10%, 30%, and 50%. The skewness and kurtosis for these distributions is listed in Table 2. In the SOL, there is a significant increase in the median MUAP amplitude between 10% and 50% (p < 0.001) and 30% and 50% contraction levels (p < 0.001). The median MUAP amplitude for the TA

also increases from 10% to 30% (p < 0.001), from 10% to 50% (p < 0.001), and from 30% to 50%

(p < 0.001). However, the large sample size and number of degrees of freedom may play a role

in the strength of significance seen.

Muscle	%MVT	Skewness	Kurtosis
Soleus	10	1.70	6.76
	30	1.91	9.40
	50	0.82	3.26
TA	10	1.14	3.54
	30	1.14	5.18
	50	0.43	2.38

Table 2. MUAP RMS amplitude distributions
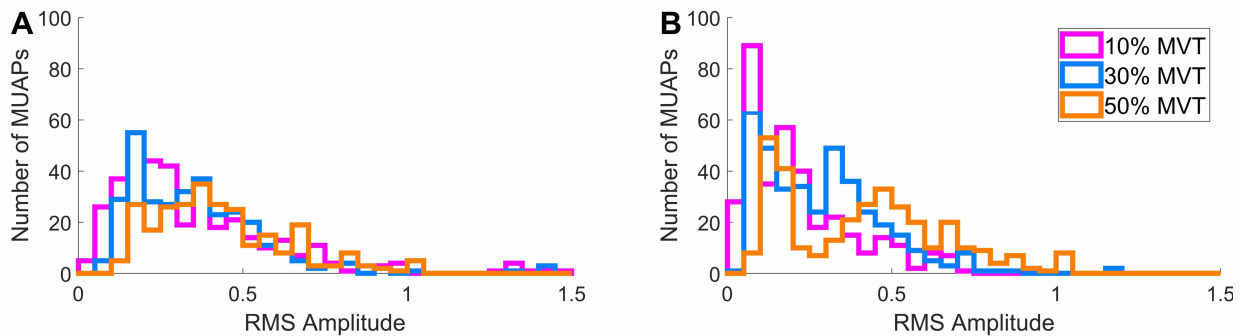
Figure 4. Distribution of MUAP RMS amplitude for the soleus and TA collected ruing 10%, 30%, and 50% MVT.

Discussion

By comparing the number of motor units decomposed in various muscles and different effort

levels and contraction speeds, this study highlights some of the protocol dependent limitations

inherent in the current implementation of high-density surface EMG decomposition. In

particular, the action potentials of lower-threshold motor units seem to be more difficult to

discriminate during relatively fast ramp contractions at high contraction levels.

Based on the current understanding of motor unit properties and previous fine wire findings,

we would expect that the number of units recruited would be skewed toward lower threshold

units for both muscles (Feiereisen et al., 1997; Kukulka & Clamann, 1981; Milner-Brown et al.,

1972; Oya et al., 2009; van Groeningen & Erkelens, 1994). However, as seen in Figure 3 our

results show that low threshold motor units can be decomposed well during slower

contractions at lower effort levels, but, as the contraction speed and effort level increase the

number of low threshold motor units discriminated was reduced. Instead, at higher contraction

speeds and torque levels we see broader distributions of recruitment thresholds. Recruitment

threshold distributions (Table 1) show that except for the TA at 10% MVT, every MVT level for

the SOL and TA show broad distribution (Kurtosis < 3.0).

The results in figure 4 show that surface decomposition produced wide range of MUAP

amplitudes. As muscle contraction level increases, larger units are recruited (HENNEMAN et al.,

1965). Additionally, it has been shown that later recruited units have larger MUAP amplitudes

(Del Vecchio et al., 2017; Martinez-Valdes et al., 2018). Our results show that in both the SOL

and TA, MUAP amplitudes significantly increase during contractions of higher effort level and

speed.

This study shows that surface EMG decomposition is capable of recording a wide range of

motor units across multiple muscles, and across several different levels of contraction. These

results confirm that although surface EMG decomposition is an improved method to

decompose larger number of motor units than more traditional methods such as fine wire

electrodes, there are still limitations, namely a bias toward units with larger MUAP amplitudes during high-speed contractions at high torque levels. It is possible that interference from the number of motor units active may be playing a large role in preventing the decomposition of as many low threshold units, and previous work has shown that small deep units may not decompose as well (Holobar et al., 2009). It is also possible that the speed of contraction has affected the decomposition algorithm's ability to capture smaller units during high contraction levels. Because the duration of ramps stayed constant for all the contraction levels, the speed of contraction varied from 1% to 5% MVT per second.

In conclusion, surface EMG decomposition is a useful tool to examine large number of motor units simultaneously across varying contraction levels and muscles. The current protocol compares recruitment thresholds and MUAP amplitudes from different contraction levels, but the results cannot be generalized due to varying speed of contraction. However, these results provide evidence that investigators should take into consideration that protocols involving high contraction speed may limit the capability of decomposition algorithm to discriminate the activity of motor units with smaller MUAP amplitudes. Future work will aim to improving the algorithm to increase the number of units with smaller MUAP amplitudes detected at high contraction levels. Additionally, further experiments will focus on decomposed units collected during varying contraction levels at a fixed, slower contraction speed.

CHAPTER IV. Concluding Remarks

Although a staggering amount of evidence has shown the importance of PICs in motor control, studying them in humans has met with some challenges. This thesis used the latest EMG recording techniques, coupled with a motor unit decomposition algorithm, to observe a large number of human motor units simultaneously and estimated PICs through ΔF calculation.

The first chapter was set out to establish the flexor-extensor relationship in the ankle muscles, the soleus and the TA. Previous findings in the human upper limb showed that the extensor had higher ΔF than the flexor. After collecting and analyzing data from healthy human participants, the results unexpectedly showed that ΔF was higher in the ankle flexor (i.e., the TA) than the extensor (i.e., the soleus). The results were also consistent in both sitting and standing positions. The findings were reaffirmed by high rate of agreement between intramuscular and surface EMG spike trains. Other notable findings included no change in ΔF across different effort levels and an increase in maximum discharge rate as the effort level increased. One reason we mentioned why ΔF was larger in the TA than the soleus was the possibility of more robust expression of monoaminergic boutons in the TA motoneurons. It is also plausible that the TA motoneurons receive stronger monoaminergic inputs from the brainstem. We explored the possibility of the TA having a larger overall firing rate range than the soleus and the results showed the difference did not cause the higher ΔF in the TA.

A previous study has shown that with increasing background EMG, the H-reflex amplitude of the soleus increases (Capaday and Stein 1987; Edamura et al. 1991; Kido et al. 2004; Capaday

and Stein 1986). Also, we expected a higher force output would require more descending inputs from the brainstem which in turn will result in higher ΔF. Therefore, it was unclear why the changes in effort levels did not result in changes in ΔF values. Revill and Fuglevand previously showed an increase in rate of rise could decrease ΔF and we thought the increase in ΔF could have been masked my increase in higher muscle contraction speeds during higher effort levels (Revill & Fuglevand, 2011).

We tested our hypothesis that increasing muscle contraction speed would decrease ΔF and the results showed that it actually did not affect ΔF. However, it generally increased initial and final discharge rates while did not influence the max discharge rates. These results were observed in both averaged data and individual unit data that were tracked across different contraction speeds. The difference between our finding and previous studies could be due to methods (Revill & Fuglevand, 2011 – a computer simulation; Vandenberk & Kalmar, 2014 – intramuscular EMG).

The increase in the initial discharge rates could be explained by a subthreshold activation of PICs, especially in smaller units (Afshariopour et al. 2020). This could potentially also explain why did not see changes in ΔF across different muscle contraction speeds. However, combined with the fact that higher muscle contraction speeds did not result in higher maximum discharge rates, it was concluded that increasing muscle contraction speeds did not increase overall descending inputs to the motoneuron pool.

In cat preparations, Wienecke and colleagues observed lower firing rates at de-recruitment than recruitment during triangular current injections (Wienecke et al., 2009). They suggested a calcium buildup after an extended period action potential as a reason behind a prolongation of the AHP. In our experiments, the ramp durations were much shorter during fast contractions compared to slow ones and it could have led to a less-buildup in calcium at the site of channels. This could result in a shorter prolongation of the AHP duration and an increase in final firing rates.

The third chapter took a deeper look into the high-density surface EMG decomposition method and highlighted some of the protocol dependent limitations. After carefully analyzing data from five healthy young participants, the results showed that the action potentials of lower-threshold motor units seemed to be more difficult to discriminate during fast ramp contractions at high effort levels. These were alarming because based on previous studies, we expected the number of units recruited would be biased toward lower threshold units (Feiereisen et al., 1997; Kukulka & Clamann, 1981; Milner-Brown et al., 1972; Oya et al., 2009; van Groeningen & Erkelens, 1994). We concluded that although surface EMG decomposition is a useful tool to examine a large number of motor units, investigators should be aware that protocols with high contraction speeds may limit the decomposition algorithm's capability to discriminate motor units with smaller amplitudes.

This dissertation was the first attempt to gain a deeper understanding of PICs in humans using high-density surface array electrodes and decomposition algorithms to record a large number of motor units simultaneously. The results from chapter one and two showed that ΔF stays

constant under various conditions, such as changing effort levels and muscle contraction speeds. These results also suggested that making these changes do not affect the amount of monoaminergic inputs from the brainstem. However, as shown in the third chapter, there is an inherent limitation with protocols involving high contraction speeds and it is possible that the decomposition algorithm's bias toward high threshold units confounded the findings from two previous chapters. Therefore, researchers should consider such limitation in designing experiments involving high contraction speeds.

CHAPTER V. References

Adrian, E. D., & Bronk, D. W. (1929). The discharge of impulses in motor nerve fibres: Part II. The frequency of discharge in reflex and voluntary contractions. *J Physiol, 67*(2), i3-151.

Afsharipour, B., Manzur, N., Duchcherer, J., Fenrich, K. F., Thompson, C. K., Negro, F., . . . Gorassini, M. A. (2020). Estimation of self-sustained activity produced by persistent inward currents using firing rate profiles of multiple motor units in humans. *J Neurophysiol, 124*(1), 63-85. doi:10.1152/jn.00194.2020

Ashworth, B., Grimby, L., & Kugelberg, E. (1967). Comparison of voluntary and reflex activation of motor units. Functional organization of motor neurones. *J Neurol Neurosurg Psychiatry, 30*(2), 91-98. doi:10.1136/jnnp.30.2.91

BASMAJIAN, J. V., & STECKO, G. (1963). THE ROLE OF MUSCLES IN ARCH SUPPORT OF THE FOOT. *J Bone Joint Surg Am, 45*, 1184-1190.

Bennett, D. J., Hultborn, H., Fedirchuk, B., & Gorassini, M. (1998). Synaptic activation of plateaus in hindlimb motoneurons of decerebrate cats. *J Neurophysiol, 80*(4), 2023-2037. doi:10.1152/jn.1998.80.4.2023

Bennett, D. J., Li, Y., Harvey, P. J., & Gorassini, M. (2001). Evidence for plateau potentials in tail motoneurons of awake chronic spinal rats with spasticity. *J Neurophysiol, 86*(4), 1972-1982. doi:10.1152/jn.2001.86.4.1972

Bennett, D. J., Li, Y., & Siu, M. (2001). Plateau potentials in sacrocaudal motoneurons of chronic spinal rats, recorded in vitro. *J Neurophysiol, 86*(4), 1955-1971. doi:10.1152/jn.2001.86.4.1955

BIGLAND, B., & LIPPOLD, O. C. (1954a). Motor unit activity in the voluntary contraction of human muscle. *J Physiol, 125*(2), 322-335. doi:10.1113/jphysiol.1954.sp005161

BIGLAND, B., & LIPPOLD, O. C. (1954b). The relation between force, velocity and integrated electrical activity in human muscles. *J Physiol, 123*(1), 214-224. doi:10.1113/jphysiol.1954.sp005044

Binder, M. D. (2003). Intrinsic dendritic currents make a major contribution to the control of motoneurone discharge. *J Physiol, 552*(Pt 3), 665. doi:10.1113/jphysiol.2003.054817

Binder, M. D., Powers, R. K., & Heckman, C. J. (2020). Nonlinear Input-Output Functions of Motoneurons. *Physiology (Bethesda), 35*(1), 31-39. doi:10.1152/physiol.00026.2019

Boccia, G., Martinez-Valdes, E., Negro, F., Rainoldi, A., & Falla, D. (2019). Motor unit discharge rate and the estimated synaptic input to the vasti muscles is higher in open compared with closed kinetic chain exercise. *J Appl Physiol (1985), 127*(4), 950-958. doi:10.1152/japplphysiol.00310.2019

Booth, V., Rinzel, J., & Kiehn, O. (1997). Compartmental model of vertebrate motoneurons for Ca2+-dependent spiking and plateau potentials under pharmacological treatment. *J Neurophysiol, 78*(6), 3371-3385. doi:10.1152/jn.1997.78.6.3371

Bracchi, F., Decandia, M., & Gualtierotti, T. (1966). Frequency stabilization in the motor centers of spinal cord and caudal brain stem. *Am J Physiol, 210*(5), 1170-1177. doi:10.1152/ajplegacy.1966.210.5.1170

Brownstone, R. M. (2006). Beginning at the end: repetitive firing properties in the final common pathway. *Prog Neurobiol, 78*(3-5), 156-172. doi:10.1016/j.pneurobio.2006.04.002

Buchthal, F., & Schmalbruch, H. (1980). Motor unit of mammalian muscle. *Physiol Rev, 60*(1), 90-142. doi:10.1152/physrev.1980.60.1.90

Burke, R. E., & Tsairis, P. (1973). Anatomy and innervation ratios in motor units of cat gastrocnemius. *J Physiol, 234*(3), 749-765. doi:10.1113/jphysiol.1973.sp010370

Button, D. C., Gardiner, K., Marqueste, T., & Gardiner, P. F. (2006). Frequency-current relationships of rat hindlimb alpha-motoneurones. *J Physiol, 573*(Pt 3), 663-677. doi:10.1113/jphysiol.2006.107292

Carlin, K. P., Jiang, Z., & Brownstone, R. M. (2000). Characterization of calcium currents in functionally mature mouse spinal motoneurons. *Eur J Neurosci, 12*(5), 1624-1634. doi:10.1046/j.1460-9568.2000.00050.x

Carlin, K. P., Jones, K. E., Jiang, Z., Jordan, L. M., & Brownstone, R. M. (2000). Dendritic L-type calcium currents in mouse spinal motoneurons: implications for bistability. *Eur J Neurosci, 12*(5), 1635-1646. doi:10.1046/j.1460-9568.2000.00055.x

Conway, B. A., Hultborn, H., Kiehn, O., & Mintz, I. (1988). Plateau potentials in alpha-motoneurones induced by intravenous injection of L-dopa and clonidine in the spinal cat. *J Physiol, 405*, 369-384. doi:10.1113/jphysiol.1988.sp017337

De Luca, C. J., Adam, A., Wotiz, R., Gilmore, L. D., & Nawab, S. H. (2006). Decomposition of surface EMG signals. *J Neurophysiol, 96*(3), 1646-1657. doi:10.1152/jn.00009.2006

De Luca, C. J., & Contessa, P. (2012). Hierarchical control of motor units in voluntary contractions. *J Neurophysiol, 107*(1), 178-195. doi:10.1152/jn.00961.2010

De Luca, C. J., & Erim, Z. (1994). Common drive of motor units in regulation of muscle force. *Trends Neurosci, 17*(7), 299-305.

De Luca, C. J., LeFever, R. S., McCue, M. P., & Xenakis, A. P. (1982). Behaviour of human motor units in different muscles during linearly varying contractions. *J Physiol, 329*, 113-128.

Del Vecchio, A., Negro, F., Felici, F., & Farina, D. (2017). Associations between motor unit action potential parameters and surface EMG features. *J Appl Physiol (1985), 123*(4), 835-843. doi:10.1152/japplphysiol.00482.2017

Denny-Brown, D., & Pennybacker, J. B. (1938). Fibrillation and fasciculation in voluntary muscle. In (Vol. 61, pp. 311-312): Brain.

Desmedt, J. E., & Godaux, E. (1976). Habituation of exteroceptive suppression and of exteroceptive reflexes in man as influenced by voluntary contraction. *Brain Res, 106*(1), 21-29. doi:10.1016/0006-8993(76)90070-6

Duchateau, J., & Enoka, R. M. (2011). Human motor unit recordings: origins and insight into the integrated motor system. *Brain Res, 1409*, 42-61. doi:10.1016/j.brainres.2011.06.011

Elbasiouny, S. M., Bennett, D. J., & Mushahwar, V. K. (2006). Simulation of Ca2+ persistent inward currents in spinal motoneurones: mode of activation and integration of synaptic inputs. *J Physiol, 570*(Pt 2), 355-374. doi:10.1113/jphysiol.2005.099119

Enoka, R. M., & Fuglevand, A. J. (2001). Motor unit physiology: some unresolved issues. *Muscle Nerve, 24*(1), 4-17. doi:10.1002/1097-4598(200101)24:1<4::aid-mus13>3.0.co;2-f

Farina, D., Arendt-Nielsen, L., Merletti, R., & Graven-Nielsen, T. (2002). Assessment of single motor unit conduction velocity during sustained contractions of the tibialis anterior muscle with advanced spike triggered averaging. *J Neurosci Methods, 115*(1), 1-12. doi:10.1016/s0165-0270(01)00510-6

Feiereisen, P., Duchateau, J., & Hainaut, K. (1997). Motor unit recruitment order during voluntary and electrically induced contractions in the tibialis anterior. *Exp Brain Res, 114*(1), 117-123. doi:10.1007/pl00005610

Foley, R. C. A., & Kalmar, J. M. (2019). Estimates of persistent inward current in human motor neurons during postural sway. *J Neurophysiol, 122*(5), 2095-2110. doi:10.1152/jn.00254.2019

Fuglevand, A. J., Lester, R. A., & Johns, R. K. (2015). Distinguishing intrinsic from extrinsic factors underlying firing rate saturation in human motor units. *J Neurophysiol, 113*(5), 1310-1322. doi:10.1152/jn.00777.2014

Gorassini, M., Bennett, D. J., Kiehn, O., Eken, T., & Hultborn, H. (1999). Activation patterns of hindlimb motor units in the awake rat and their relation to motoneuron intrinsic properties. *J Neurophysiol, 82*(2), 709-717. doi:10.1152/jn.1999.82.2.709

Gorassini, M., Eken, T., Bennett, D. J., Kiehn, O., & Hultborn, H. (2000). Activity of hindlimb motor units during locomotion in the conscious rat. *J Neurophysiol, 83*(4), 2002-2011. doi:10.1152/jn.2000.83.4.2002

Gorassini, M., Yang, J. F., Siu, M., & Bennett, D. J. (2002). Intrinsic activation of human motoneurons: possible contribution to motor unit excitation. *J Neurophysiol, 87*(4), 1850-1858. doi:10.1152/jn.00024.2001

Gorassini, M. A., Knash, M. E., Harvey, P. J., Bennett, D. J., & Yang, J. F. (2004). Role of motoneurons in the generation of muscle spasms after spinal cord injury. *Brain, 127*(Pt 10), 2247-2258. doi:10.1093/brain/awh243

Granit, R., Kernell, D., & Lamarre, Y. (1966). Synaptic stimulation superimposed on motoneurones firing in the 'secondary range' to injected current. *J Physiol, 187*(2), 401-415. doi:10.1113/jphysiol.1966.sp008098

Grimby, L., & Hannerz, J. (1968). Recruitment order of motor units on voluntary contraction: changes induced by proprioceptive afferent activity. *J Neurol Neurosurg Psychiatry, 31*(6), 565-573. doi:10.1136/jnnp.31.6.565

Grimby, L., & Hannerz, J. (1970). Differences in recruitment order of motor units in phasic and tonic flexion reflex in "spinal man". *J Neurol Neurosurg Psychiatry, 33*(5), 562-570. doi:10.1136/jnnp.33.5.562

Gydikov, A., & Kosarov, D. (1974). Influence of various factors on the length of the summated depolarized area of the muscle fibres in voluntary activating of motor units and electrical stimulation. *Electromyogr Clin Neurophysiol, 14*(1), 79-93.

Gydikov, A., Kosarov, D., Tankov, N., & Shapkov, U. T. (1973). Human alpha motoneuron and motor unit discharges in voluntary muscle contraction. *Agressologie, 14 Spec B*(0), 23-34.

Harvey, P. J., Li, X., Li, Y., & Bennett, D. J. (2006a). 5-HT2 receptor activation facilitates a persistent sodium current and repetitive firing in spinal motoneurons of rats with and without chronic spinal cord injury. *J Neurophysiol, 96*(3), 1158-1170. doi:10.1152/jn.01088.2005

Harvey, P. J., Li, X., Li, Y., & Bennett, D. J. (2006b). Endogenous monoamine receptor activation is essential for enabling persistent sodium currents and repetitive firing in rat spinal motoneurons. *J Neurophysiol, 96*(3), 1171-1186. doi:10.1152/jn.00341.2006

Hassan, A., Thompson, C. K., Negro, F., Cummings, M., Powers, R. K., Heckman, C. J., . . . McPherson, L. M. (2020). Impact of parameter selection on estimates of motoneuron excitability using paired motor unit analysis. *J Neural Eng, 17*(1), 016063. doi:10.1088/1741-2552/ab5eda

Heckman, C. J., & Binder, M. D. (1988). Analysis of effective synaptic currents generated by homonymous Ia afferent fibers in motoneurons of the cat. *J Neurophysiol, 60*(6), 1946-1966. doi:10.1152/jn.1988.60.6.1946

Heckman, C. J., & Binder, M. D. (1991). Analysis of Ia-inhibitory synaptic input to cat spinal motoneurons evoked by vibration of antagonist muscles. *J Neurophysiol, 66*(6), 1888-1893. doi:10.1152/jn.1991.66.6.1888

Heckman, C. J., & Binder, M. D. (1993). Computer simulations of the effects of different synaptic input systems on motor unit recruitment. *J Neurophysiol, 70*(5), 1827-1840. doi:10.1152/jn.1993.70.5.1827

Heckman, C. J., & Enoka, R. M. (2012). Motor unit. *Compr Physiol, 2*(4), 2629-2682. doi:10.1002/cphy.c100087

Heckman, C. J., Johnson, M., Mottram, C., & Schuster, J. (2008). Persistent inward currents in spinal motoneurons and their influence on human motoneuron firing patterns. *Neuroscientist, 14*(3), 264-275. doi:10.1177/1073858408314986

Heckman, C. J., Lee, R. H., & Brownstone, R. M. (2003). Hyperexcitable dendrites in motoneurons and their neuromodulatory control during motor behavior. *Trends Neurosci, 26*(12), 688-695. doi:10.1016/j.tins.2003.10.002

Heckman, C. J., Mottram, C., Quinlan, K., Theiss, R., & Schuster, J. (2009). Motoneuron excitability: the importance of neuromodulatory inputs. *Clin Neurophysiol, 120*(12), 2040-2054. doi:10.1016/j.clinph.2009.08.009

Heckmann, C. J., Gorassini, M. A., & Bennett, D. J. (2005). Persistent inward currents in motoneuron dendrites: implications for motor output. *Muscle Nerve, 31*(2), 135-156. doi:10.1002/mus.20261

Henneman, E., & Mendell, L. M. (1981). Functional organization of motoneuron pool and its inputs. In (pp. 423-507): American Physiological Society

In V. B. Brooks (Ed.) *Handbook of Physiology, The Nervous System, Motor Control*.

HENNEMAN, E., SOMJEN, G., & CARPENTER, D. O. (1965). FUNCTIONAL SIGNIFICANCE OF CELL SIZE IN SPINAL MOTONEURONS. *J Neurophysiol, 28*, 560-580. doi:10.1152/jn.1965.28.3.560

Hill, A. V. (1936). Excitation and accommodation in nerve. In (Vol. 119): The Royal Society.

Holobar, A., Farina, D., Gazzoni, M., Merletti, R., & Zazula, D. (2009). Estimating motor unit discharge patterns from high-density surface electromyogram. *Clin Neurophysiol, 120*(3), 551-562. doi:10.1016/j.clinph.2008.10.160

Holobar, A., Minetto, M. A., Botter, A., Negro, F., & Farina, D. (2010). Experimental analysis of accuracy in the identification of motor unit spike trains from high-density surface EMG. *IEEE Trans Neural Syst Rehabil Eng, 18*(3), 221-229. doi:10.1109/TNSRE.2010.2041593

Holobar, A., Minetto, M. A., & Farina, D. (2014). Accurate identification of motor unit discharge patterns from high-density surface EMG and validation with a novel signal-based performance metric. *J Neural Eng, 11*(1), 016008.

Hounsgaard, J., Hultborn, H., Jespersen, B., & Kiehn, O. (1984). Intrinsic membrane properties causing a bistable behaviour of alpha-motoneurones. *Exp Brain Res, 55*(2), 391-394. doi:10.1007/BF00237290

Hounsgaard, J., Hultborn, H., Jespersen, B., & Kiehn, O. (1988). Bistability of alpha-motoneurones in the decerebrate cat and in the acute spinal cat after intravenous 5-hydroxytryptophan. *J Physiol, 405*, 345-367.

Hounsgaard, J., & Kiehn, O. (1985). Ca++ dependent bistability induced by serotonin in spinal motoneurons. *Exp Brain Res, 57*(2), 422-425. doi:10.1007/BF00236551

Hounsgaard, J., & Kiehn, O. (1989). Serotonin-induced bistability of turtle motoneurones caused by a nifedipine-sensitive calcium plateau potential. *J Physiol, 414*, 265-282. doi:10.1113/jphysiol.1989.sp017687

Hounsgaard, J., & Kiehn, O. (1993). Calcium spikes and calcium plateaux evoked by differential polarization in dendrites of turtle motoneurones in vitro. *J Physiol, 468*, 245-259. doi:10.1113/jphysiol.1993.sp019769

Hounsgaard, J., Kiehn, O., & Mintz, I. (1988). Response properties of motoneurones in a slice preparation of the turtle spinal cord. *J Physiol, 398*, 575-589. doi:10.1113/jphysiol.1988.sp017058

Hultborn, H. (2002). Plateau potentials and their role in regulating motoneuronal firing. *Adv Exp Med Biol, 508*, 213-218. doi:10.1007/978-1-4615-0713-0_26

Hultborn, H., Brownstone, R. B., Toth, T. I., & Gossard, J. P. (2004). Key mechanisms for setting the input-output gain across the motoneuron pool. *Prog Brain Res, 143*, 77-95. doi:10.1016/s0079-6123(03)43008-2

Johnson, M. D., & Heckman, C. J. (2010). Interactions between focused synaptic inputs and diffuse neuromodulation in the spinal cord. *Ann N Y Acad Sci, 1198*, 35-41. doi:10.1111/j.1749-6632.2010.05430.x

Johnson, M. D., & Heckman, C. J. (2014). Gain control mechanisms in spinal motoneurons. *Front Neural Circuits, 8*, 81. doi:10.3389/fncir.2014.00081

Johnson, M. D., Thompson, C. K., Tysseling, V. M., Powers, R. K., & Heckman, C. J. (2017). The potential for understanding the synaptic organization of human motor commands via the firing patterns of motoneurons. *J Neurophysiol, 118*(1), 520-531. doi:10.1152/jn.00018.2017

Kanosue, K., Yoshida, M., Akazawa, K., & Fujii, K. (1979). The number of active motor units and their firing rates in voluntary contraction of human brachialis muscle. *Jpn J Physiol, 29*(4), 427-443. doi:10.2170/jjphysiol.29.427

Kernell, D. (2006). *Motoneurone and its Muscle Fibres*: Oxford Scholarships Online.

Kiehn, O., & Eken, T. (1998). Functional role of plateau potentials in vertebrate motor neurons. *Curr Opin Neurobiol, 8*(6), 746-752. doi:10.1016/s0959-4388(98)80117-7

Kiehn, O., Erdal, J., Eken, T., & Bruhn, T. (1996). Selective depletion of spinal monoamines changes the rat soleus EMG from a tonic to a more phasic pattern. *J Physiol, 492 (Pt 1)*, 173-184.

Kim, E. H., Wilson, J. M., Thompson, C. K., & Heckman, C. J. (2020). Differences in estimated persistent inward currents between ankle flexors and extensors in humans. *J Neurophysiol, 124*(2), 525-535. doi:10.1152/jn.00746.2019

Krnjević, K., Puil, E., & Werman, R. (1978). EGTA and motoneuronal after-potentials. *J Physiol, 275*, 199-223. doi:10.1113/jphysiol.1978.sp012186

Kukulka, C. G., & Clamann, H. P. (1981). Comparison of the recruitment and discharge properties of motor units in human brachial biceps and adductor pollicis during isometric contractions. *Brain Res, 219*(1), 45-55. doi:10.1016/0006-8993(81)90266-3

Lee, R. H., & Heckman, C. J. (1996). Influence of voltage-sensitive dendritic conductances on bistable firing and effective synaptic current in cat spinal motoneurons in vivo. *J Neurophysiol, 76*(3), 2107-2110. doi:10.1152/jn.1996.76.3.2107

Lee, R. H., & Heckman, C. J. (1998a). Bistability in spinal motoneurons in vivo: systematic variations in persistent inward currents. *J Neurophysiol, 80*(2), 583-593. doi:10.1152/jn.1998.80.2.583

Lee, R. H., & Heckman, C. J. (1998b). Bistability in spinal motoneurons in vivo: systematic variations in rhythmic firing patterns. *J Neurophysiol, 80*(2), 572-582. doi:10.1152/jn.1998.80.2.572

Lee, R. H., & Heckman, C. J. (1999). Enhancement of bistability in spinal motoneurons in vivo by the noradrenergic alpha1 agonist methoxamine. *J Neurophysiol, 81*(5), 2164-2174. doi:10.1152/jn.1999.81.5.2164

Lee, R. H., & Heckman, C. J. (2000). Adjustable amplification of synaptic input in the dendrites of spinal motoneurons in vivo. *J Neurosci, 20*(17), 6734-6740.

Li, X., Murray, K., Harvey, P. J., Ballou, E. W., & Bennett, D. J. (2007). Serotonin facilitates a persistent calcium current in motoneurons of rats with and without chronic spinal cord injury. *J Neurophysiol, 97*(2), 1236-1246. doi:10.1152/jn.00995.2006

Li, Y., & Bennett, D. J. (2003). Persistent sodium and calcium currents cause plateau potentials in motoneurons of chronic spinal rats. *J Neurophysiol, 90*(2), 857-869. doi:10.1152/jn.00236.2003

Li, Y., Gorassini, M. A., & Bennett, D. J. (2004). Role of persistent sodium and calcium currents in motoneuron firing and spasticity in chronic spinal rats. *J Neurophysiol, 91*(2), 767-783. doi:10.1152/jn.00788.2003

Liddell, E. G. T., & Sherrington, C. S. (1925). Further Observation on Myotatic Reflexes. In (Vol. Series B, pp. 267–283): Royal Society of London. Proceedings. *Containing Papers of a Biological Character*.

Lindsay, A. D., & Binder, M. D. (1991). Distribution of effective synaptic currents underlying recurrent inhibition in cat triceps surae motoneurons. *J Neurophysiol, 65*(2), 168-177. doi:10.1152/jn.1991.65.2.168

Manuel, M., Meunier, C., Donnet, M., & Zytnicki, D. (2007). Resonant or not, two amplification modes of proprioceptive inputs by persistent inward currents in spinal motoneurons. *J Neurosci, 27*(47), 12977-12988. doi:10.1523/JNEUROSCI.3299-07.2007

Martinez-Valdes, E., Negro, F., Falla, D., De Nunzio, A. M., & Farina, D. (2018). Surface electromyographic amplitude does not identify differences in neural drive to synergistic muscles. *J Appl Physiol (1985), 124*(4), 1071-1079. doi:10.1152/japplphysiol.01115.2017

Martinez-Valdes, E., Negro, F., Falla, D., Dideriksen, J. L., Heckman, C. J., & Farina, D. (2020). Inability to increase the neural drive to muscle is associated with task failure during submaximal contractions. *J Neurophysiol, 124*(4), 1110-1121. doi:10.1152/jn.00447.2020

Martinez-Valdes, E., Negro, F., Farina, D., & Falla, D. (2020). Divergent response of low- versus high-threshold motor units to experimental muscle pain. *J Physiol, 598*(11), 2093-2108. doi:10.1113/JP279225

Martinez-Valdes, E., Negro, F., Laine, C. M., Falla, D., Mayer, F., & Farina, D. (2017). Tracking motor units longitudinally across experimental sessions with high-density surface electromyography. *J Physiol, 595*(5), 1479-1496. doi:10.1113/JP273662

Meehan, C. F., Sukiasyan, N., Zhang, M., Nielsen, J. B., & Hultborn, H. (2010). Intrinsic properties of mouse lumbar motoneurons revealed by intracellular recording in vivo. *J Neurophysiol, 103*(5), 2599-2610. doi:10.1152/jn.00668.2009

Mendell, L. M., & Henneman, E. (1968). Terminals of single Ia fibers: distribution within a pool of 300 homonymous motor neurons. *Science, 160*(3823), 96-98. doi:10.1126/science.160.3823.96

Mendell, L. M., & Henneman, E. (1971). Terminals of single Ia fibers: location, density, and distribution within a pool of 300 homonymous motoneurons. *J Neurophysiol, 34*(1), 171-187. doi:10.1152/jn.1971.34.1.171

Miller, J. F., Paul, K. D., Lee, R. H., Rymer, W. Z., & Heckman, C. J. (1996). Restoration of extensor excitability in the acute spinal cat by the 5-HT2 agonist DOI. *J Neurophysiol, 75*(2), 620-628. doi:10.1152/jn.1996.75.2.620

Milner-Brown, H. S., Stein, R. B., & Yemm, R. (1972). Mechanisms for increased force during voluntary contractions. *J Physiol, 226*(2), 18P-19P.

Milner-Brown, H. S., Stein, R. B., & Yemm, R. (1973). The orderly recruitment of human motor units during voluntary isometric contractions. *J Physiol, 230*(2), 359-370. doi:10.1113/jphysiol.1973.sp010192

Monster, A. W., & Chan, H. (1977). Isometric force production by motor units of extensor digitorum communis muscle in man. *J Neurophysiol, 40*(6), 1432-1443. doi:10.1152/jn.1977.40.6.1432

Mottram, C. J., Suresh, N. L., Heckman, C. J., Gorassini, M. A., & Rymer, W. Z. (2009). Origins of abnormal excitability in biceps brachii motoneurons of spastic-paretic stroke survivors. *J Neurophysiol, 102*(4), 2026-2038. doi:10.1152/jn.00151.2009

Nawab, S. H., Chang, S. S., & De Luca, C. J. (2010). High-yield decomposition of surface EMG signals. *Clin Neurophysiol, 121*(10), 1602-1615. doi:10.1016/j.clinph.2009.11.092

Negro, F., Muceli, S., Castronovo, A. M., Holobar, A., & Farina, D. (2016). Multi-channel intramuscular and surface EMG decomposition by convolutive blind source separation. *J Neural Eng, 13*(2), 026027. doi:10.1088/1741-2560/13/2/026027

Oya, T., Riek, S., & Cresswell, A. G. (2009). Recruitment and rate coding organisation for soleus motor units across entire range of voluntary isometric plantar flexions. *J Physiol, 587*(Pt 19), 4737-4748. doi:10.1113/jphysiol.2009.175695

Perrier, J. F., & Hounsgaard, J. (2003). 5-HT2 receptors promote plateau potentials in turtle spinal motoneurons by facilitating an L-type calcium current. *J Neurophysiol, 89*(2), 954-959. doi:10.1152/jn.00753.2002

Piper, H. (1912). Electrophysiologie Menschlicher Muskeln. In. Berlin: Springer-Verlag.

Powers, R. K., & Binder, M. D. (2001). Input-output functions of mammalian motoneurons. *Rev Physiol Biochem Pharmacol, 143*, 137-263.

Powers, R. K., & Heckman, C. J. (2015). Contribution of intrinsic motoneuron properties to discharge hysteresis and its estimation based on paired motor unit recordings: a simulation study. *J Neurophysiol, 114*(1), 184-198. doi:10.1152/jn.00019.2015

Powers, R. K., Nardelli, P., & Cope, T. C. (2008). Estimation of the contribution of intrinsic currents to motoneuron firing based on paired motoneuron discharge records in the decerebrate cat. *J Neurophysiol, 100*(1), 292-303. doi:10.1152/jn.90296.2008

Revill, A. L., & Fuglevand, A. J. (2011). Effects of persistent inward currents, accommodation, and adaptation on motor unit behavior: a simulation study. *J Neurophysiol, 106*(3), 1467-1479. doi:10.1152/jn.00419.2011

Schwindt, P., & Crill, W. E. (1977). A persistent negative resistance in cat lumbar motoneurons. *Brain Res, 120*(1), 173-178. doi:10.1016/0006-8993(77)90510-8

Schwindt, P. C., & Crill, W. E. (1981). Voltage clamp study of cat spinal motoneurons during strychnine-induced seizures. *Brain Res, 204*(1), 226-230. doi:10.1016/0006-8993(81)90669-7

Schwindt, P. C., Spain, W., & Crill, W. E. (1984). Epileptogenic action of tungstic acid gel on cat lumbar motoneurons. *Brain Res, 291*(1), 140-144. doi:10.1016/0006-8993(84)90660-7

Shapiro, M. S., Gomeza, J., Hamilton, S. E., Hille, B., Loose, M. D., Nathanson, N. M., . . . Wess, J. (2001). Identification of subtypes of muscarinic receptors that regulate Ca2+ and K+ channel activity in sympathetic neurons. *Life Sci, 68*(22-23), 2481-2487. doi:10.1016/s0024-3205(01)01042-6

Steeves, J. D., & Jordan, L. M. (1980). Localization of a descending pathway in the spinal cord which is necessary for controlled treadmill locomotion. *Neurosci Lett, 20*(3), 283-288.

Stephenson, J. L., & Maluf, K. S. (2011). Dependence of the paired motor unit analysis on motor unit discharge characteristics in the human tibialis anterior muscle. *J Neurosci Methods, 198*(1), 84-92. doi:10.1016/j.jneumeth.2011.03.018

Thompson, C. K., Negro, F., Johnson, M. D., Holmes, M. R., McPherson, L. M., Powers, R. K., . . . Heckman, C. J. (2018). Robust and accurate decoding of motoneuron behaviour and prediction of the resulting force output. *J Physiol, 596*(14), 2643-2659. doi:10.1113/JP276153

Trajano, G. S., Taylor, J. L., Orssatto, L. B. R., McNulty, C. R., & Blazevich, A. J. (2020). Passive muscle stretching reduces estimates of persistent inward current strength in soleus motor units. *J Exp Biol, 223*(Pt 21). doi:10.1242/jeb.229922

Turkin, V. V., O'Neill, D., Jung, R., Iarkov, A., & Hamm, T. M. (2010). Characteristics and organization of discharge properties in rat hindlimb motoneurons. *J Neurophysiol, 104*(3), 1549-1565. doi:10.1152/jn.00379.2010

van Groeningen, C. J., & Erkelens, C. J. (1994). Task-dependent differences between mono- and bi-articular heads of the triceps brachii muscle. *Exp Brain Res, 100*(2), 345-352. doi:10.1007/BF00227204

Vandenberk, M. S., & Kalmar, J. M. (2014). An evaluation of paired motor unit estimates of persistent inward current in human motoneurons. *J Neurophysiol, 111*(9), 1877-1884. doi:10.1152/jn.00469.2013

Wachholder, K. (1928). Willkürliche Haltung und Bewegung: Insbesondere im Lichte elektrophysiologischer Untersuchungen. In (Vol. 26, pp. 568-775): Ergebnisse der Physiologie.

Wienecke, J., Zhang, M., & Hultborn, H. (2009). A prolongation of the postspike afterhyperpolarization following spike trains can partly explain the lower firing rates at derecruitment than those at recruitment. *J Neurophysiol, 102*(6), 3698-3710. doi:10.1152/jn.90995.2008

Wigton, R. S., & Brink, F. (1944). STUDIES OF ACCOMMODATION OF NERVE IN PARATHYROID DEFICIENCY. *J Clin Invest, 23*(6), 898-903. doi:10.1172/JCI101564

Wilson, J. M., Thompson, C. K., Miller, L. C., & Heckman, C. J. (2015). Intrinsic excitability of human motoneurons in biceps brachii versus triceps brachii. *J Neurophysiol, 113*(10), 3692-3699. doi:10.1152/jn.00960.2014